

**EFFECT OF THERMAL AGEING ON Al ALLOY METAL  
MATRIX COMPOSITE**

Thesis submitted in the partial fulfillment of the requirements for the award of

the Degree of

**MASTER OF ENGINEERING**

**IN**

**(PRODUCTION AND INDUSTRIAL ENGINEERING)**

Submitted By:

**Narinder Singh**

**Registration No: 800882006**

Under the supervision of:

**Mr. Kishore Khanna**

**Assistant Professor, MED**

**Dr. Shweta Goyal**

**Assistant professor, CED**



**MECHANICAL ENGINEERING DEPARTMENT**

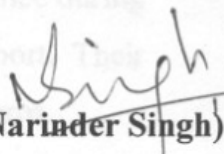
**THAPAR UNIVERSITY, PATIALA**

JULY 2010


## DECLARATION

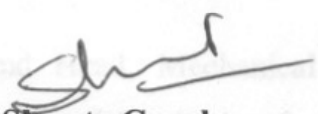
---

I here by declare that thesis entitled “EFFECT OF THERMAL AGEING ON AL ALLOY METAL MATRIX COMPOSITE” is an authentic record of my study carried out as requirements for the award of degree of M.E. (Production and Industrial Engineering) at Thapar University, Patiala, under the guidance of Mr. Kishore Khanna, Assistant Professor, Thapar University, Patiala and Dr. Shweta Goyal, Assistant Professor, Civil Engineering Department, Thapar University, Patiala. The matter embodied in this thesis has not been submitted in part or full to any other university or institute for the award of any degree.


  
(Narinder Singh) 15/07/10

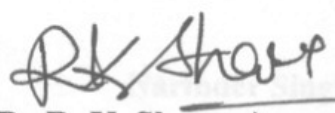
This is to certify that above declaration made by the student concerned is correct to the best of my knowledge and belief.

  
**Mr. Kishore Khanna**  
Assistant Professor  
MED, Thapar University  
Patiala-147004

  
**Dr. Shweta Goyal**  
Assistant Professor  
CED, Thapar University  
Patiala-147004

*Countersigned by:*

  
**(Dr. S.K. Mohapatra)**  
Head of Department  
Department of Mechanical Engineering  
Thapar University  
Patiala-147004

  
**(Dr. R. K. Sharma)** - -  
Dean of Academic Affairs  
Thapar University  
Patiala-147004

## ACKNOWLEDGEMENT

To achieve success in any work, guidance plays an important role. It makes us put right amount of energy in the right direction and at right time to obtain the desired result. I express my sincere gratitude to my guides, **Mr. Kishore Khanna**, Assistant Professor, Mechanical engineering department and **Dr. Shweta Goyal**, Assistant Professor, Civil Engineering Department, Thapar University, Patiala, for giving valuable guidance during the course of this work, for their ever encouraging and timely moral support. Their enormous knowledge always helped me unconditionally to solve various problems.

I am also very thankful **Dr. Rahul Chibber**, Assistant Professor, Mechanical engineering Department, Thapar Univeristy, Patiala for help me a lot during my work.

I am also grateful to my loving parents who has given me moral support at each moment during my thesis work

I am greatly thankful to **Dr. S.K. Mohapatra**, Professor and Head, Mechanical Engineering Department, Thapar University, for his encouragement and inspiration for execution of the thesis work. I express my feelings of thanks to the entire faculty and staff, Department of Mechanical Engineering, Thapar University, Patiala for their help, inspiration and moral support, which went a long way in the successful completion of my Thesis.

Last but not least, I would like to thank God for all good deeds.

**Narinder Singh**

**(Reg. No. 800882006)**

## **ABSTRACT**

Aluminium alloys are widely used in aerospace and automobile industries, due to their good mechanical properties and excellent ability, to unify the properties of ceramic phase with the metallic phase which has been useful in gearing up the extensive research activities all around the world.

Present work is focused on the study of age hardening behaviour of Aluminium LM-4/ Zircon sand composite produced by the stir casting technique. Water and Brine solution has been used as the quenching media. Thermal ageing has been done at different temperature, time and quenching media. Microhardness and wear tests were performed on the samples obtained from the stir casting process. The results of ageing demonstrate that the microhardness of the composite depend on the quenching medium in which they are heat treated. Scanning Electron Microscopy of the samples was conducted to analyze the distribution pattern of the reinforced material in the matrix alloy. X-ray Diffraction was performed to know the presence of the phases of reinforced material.

# CONTENTS

Title	Page No.
Declaration	
Acknowledgement	i
Abstract	ii
List of figures	iii
List of tables	v
Chapter 1	
INTRODUCTION	1-16
1.1 Introduction of metal matrix composite	1
1.2 Development Objective	2
1.3 Matrix	3
1.4 Matrix material	3
1.5 Reinforcement	3
1.6 Classification of composite	4
1.6.1 Based on matrix material	4
1.6.2 Based on reinforced material structure	4
1.7 Processing	5
1.7.1 Liquid state processing	5
1.7.1.1 Stir casting	6
1.7.1.2 Infiltration	7
1.7.1.3 Gas pressure filtration	8
1.7.1.4 Squeeze casting filtration	9
1.7.1.5 Pressure die infiltration	10
1.7.2 Solid state processing	10
1.7.2.1 Diffusion bonding	11
1.7.2.2 Sintering	12
1.8 Application	15
1.9 Thermal ageing	15
Chapter 2	
LITERATURE REVIEW	17-24
Chapter 3	
PROBLEM FORMULATION	25

Chapter 4	
Experimentation	26-37
4.1 Synthesis of composite	26
4.1.1 Matrix material	26
4.1.2 Reinforcement material	26
4.2 Synthesis	27
4.2.1 Stirrer design	28
4.2.2 Particulate preheating temperature	28
4.2.3 Stirring speed	28
4.3 Thermal ageing	28
4.4 Quenching media	28
4.5 Experimental plan	29
4.6 Parameter matrix	30
4.7 Material testing	32
4.7.1 Micro hardness tester	32
4.7.2 Wear testing machine	33
4.8 Characterization technique	33
4.6.1 X-ray diffraction	33
4.6.2 Scanning electron microscope	35
Chapter 5	
Results and Discussions	38-50
5.1 Hardness test	38
5.2 Wear test	41
5.3 Optical micrography	44
5.4 SEM results	45
5.5 XRD results	46
5.6 Comparison between hardness and cumulative wear loss	49
5.7 Area fraction specimen by image j software	50
Chapter 6	
Conclusion	51
References	52

## List of figures

Figure No.	Page No.
Figure 1.1: Stir casting	6
Figure 1.2: Gas Pressure Infiltration	8
Figure 1.3: Squeeze Casting Infiltration	9
Figure 1.4: Pressure Die Infiltration	10
Figure 1.5: Diffusion Bonding	11
Figure 1.6: Die Fill stage	12
Figure 1.7: Hot Pressing	12
Figure 1.8: Part ejection	13
Figure 1.9: Hot Isostatic Pressing	13
Figure 1.10: Extrusion	14
Figure 4.1: Work plan	29
Figure 4.2: Stir casting set up	31
Figure 4.3: Crucible	31
Figure 4.4: Metal mould	31
Figure 4.5: Microhardness tester	32
Figure 4.6: Wear testing machine	33
Figure 4.7: Schematic for Bragg's law	34
Figure 4.8: Schematic for X-ray diffractometer	35
Figure 4.9: Schematic for scanning electron microscope	36
Figure 5.1: Microhardness of alloys and composites as a function of aging time	41
Figure 5.2: Cumulative wear loss of alloy as a function of sliding distance	42

Figure 5.3: Cumulative wear loss of composite as a function of sliding distance	43
Figure 5.4: Microstructure image of aluminum matrix at different magnifications	44
Figure 5.5: Microstructure image of aluminum matrix embedded with zircon sand particles at different magnification	44
Figure 5.6: Scanning electron micrograph of alloy without reinforcement	45
Figure 5.7: Scanning electron micrograph of alloy with reinforcement of zircon sand	46
Figure 5.8: X-ray diffraction pattern of the alloy	47
Figure 5.9: X-ray diffraction pattern of the composite	48
Figure 5.10: Comparison showing relation between hardness and wear rate	49
Figure 5.11: Images of specimen 5 using image j software	50
Figure 5.12: Images of specimen 6 using image j software	50
Figure 5.13: Images of specimen 7 using image j software	51
Figure 5.14: Images of specimen 8 using image j software	51
Figure 5.15: Comparison between area fraction and slope of cumulative wear loss	52

## **List of tables**

Table no.	Page no.
Table 4.1: Chemical composition of aluminum alloy	26
Table 4.2: Particle size of reinforcement material	26
Table 4.3: Chemical Composition of reinforcement material	27
Table 4.4: Parameter Matrix	30
Table 5.1: Microhardness data of alloy after ageing of 2 hours	38
Table 5.2: Microhardness data of composite after ageing of 2 hours	38
Table 5.3: Microhardness data of alloy after ageing of 4 hours	39
Table 5.4: Microhardness data of composite after ageing of 4 hours	39
Table 5.5: Microhardness data of alloy after ageing of 8 hours	40
Table 5.6: Microhardness data of composite after ageing of 8 hours	40
Table 5.7: Data of cumulative wear loss of alloy	42
Table 5.8: Data of cumulative wear loss of composite	43
Table 5.9: XRD results of alloy	47
Table 5.10: XRD results of alloy reinforced with zircon sand	48

### 1.1 INTRODUCTION OF METAL MATRIX COMPOSITE:

Metal matrix composite materials have found application in many areas of daily life for quite some time. Often it is not realized that the application makes use of composite materials. Metal matrix composites (MMCs), like all composites; consist of at least two chemically and physically distinct phases, suitably distributed to provide properties not obtainable with either of the individual phases. Generally, there are two phases, e.g. a fibrous or particulate phase in a metallic matrix. Examples include  $\text{Al}_2\text{O}_3$  fiber reinforced in a copper matrix for superconducting magnets; tungsten carbide (W/C) cobalt (Co) particulate composites used as cutting tool and oil drilling inserts; and SiC particle reinforced Al matrix composites used in aero space, automotive, and thermal management applications.

For many researchers the term metal matrix composites is often equated with the term light metal matrix composites (MMCs). Substantial progress in the development of light metal matrix composites has been achieved in recent decades, so that they could be introduced into the most important applications. In traffic engineering, especially in the automotive industry, MMCs have been used commercially in fiber reinforced pistons and aluminium crank cases with strengthened cylinder surfaces as well as particle-strengthened brake disks. These innovative materials open up unlimited possibilities for modern material science and development; the characteristics of MMCs can be designed into the material, custom-made, dependent on the application. From this potential, metal matrix composites fulfil all the desired conceptions of the designer [1-2]. This material group becomes interesting for use as constructional and functional materials, if the property profile of conventional materials either does not reach the increased standards of specific demands, or is the solution of the problem.

## 1.2 DEVELOPMENT OBJECTIVE:

The development objectives for metal composite materials are:

- i. Increase in yield strength and tensile strength at room temperature and above while maintaining the minimum ductility or rather toughness
- ii. Increase in creep resistance at higher temperatures compared to that of conventional alloy
- iii. Increase in fatigue strength, especially at higher temperatures
- iv. Improvement of thermal shock resistance
- v. Improvement of corrosion resistance
- vi. Increase in Young's modulus
- vii. Reduction of thermal elongation

These are advantages metal matrix composites with respect to unreinforced metals and polymer matrix composites.

Advantage with respect to unreinforced metals:

- i. Major weight savings due to strength-to weight ratio
- ii. Exceptional dimensional stability
- iii. Higher elevated temperature stability, i.e., creep resistance
- iv. Significantly improved cyclic fatigue characteristics

With respect to Polymer matrix composite, MMCs offer these advantages:

- i. Higher strength and stiffness
- ii. Higher service temperatures
- iii. Higher electrical conductivity (grounding, space charging)
- iv. Higher thermal conductivity
- v. Better transverse properties
- vi. Improved joining characteristics
- vii. Radiation survivability (laser, UV, nuclear etc.)
- viii. Little or no contamination (no out-gassing or moisture absorption problems)

### **1.3 MATRIX**

The matrix is the monolithic material into which the reinforcement is embedded, and is completely continuous. This means that there is a path through the matrix to any point in the material, unlike two materials sandwiched together. In structural applications, the matrix is usually a lighter metal such as aluminium, magnesium, or titanium, and provides a compliant support for the reinforcement. In high temperature applications, cobalt and cobalt-nickel alloy matrices are common [23].

### **1.4 MATRIX MATERIAL**

The most common matrix materials used in composite are as follows

1. Aluminium matrix
2. Copper Matrix
3. Titanium Matrix

### **1.5 REINFORCEMENT**

The reinforcement material is embedded into the matrix. The reinforcement does not always serve a purely structural task (reinforcing the compound), but is also used to change physical properties such as wear resistance, friction coefficient, or thermal conductivity. The reinforcement can be either continuous, or discontinuous. Discontinuous MMCs can be isotropic, and can be worked with standard metalworking techniques, such as extrusion, forging or rolling. In addition, they may be machined using conventional techniques, but commonly would need the use of poly crystalline diamond tooling. Continuous reinforcement uses monofilament wires or fibers such as carbon fiber or silicon carbide. Because the fibers are embedded into the matrix in a certain direction, the result is an anisotropic structure in which the alignment of the material affects its strength. One of the first MMCs used boron filament as reinforcement. Discontinuous reinforcement uses "whiskers", short fibers, or particles. The most common reinforcing materials in this category are alumina and silicon carbide.

## **1.6 CLASSIFICATION OF COMPOSITE:**

There are two classification systems of composite materials. One of them is based on the matrix material (metal, ceramic and polymer) and the second is based on the material structure:

**1.6.1 Based on matrix material:** These type of composites are based on matrix material

1. Metal Matrix Composites (MMC): Metal Matrix Composites are composed of a metallic matrix (aluminium, magnesium, iron, cobalt, copper) and a dispersed ceramic (oxides, carbides) or metallic (lead, tungsten, molybdenum) phase.
2. Ceramic Matrix Composites (CMC): Ceramic Matrix Composites are composed of a ceramic matrix and embedded fibers of other ceramic material (dispersed phase).
3. Polymer Matrix Composites (PMC): Polymer Matrix Composites are composed of a matrix from thermoset (Unsaturated Polyester (UP), Epoxy (EP)) or thermoplastic (Polycarbonate (PC), Polyvinylchloride, Nylon, Polystyrene ) and embedded glass, carbon, steel or Kevlar fibers (dispersed phase).

**1.6.2 Based on reinforced material structure:** These type of composites are based on reinforcing material structure.

1. Particulate Composites:

Particulate Composites consist of a matrix reinforced by a dispersed phase in form of particles.

- i. Composites with random orientation of particles.
- ii. Composites with preferred orientation of particles. Dispersed phase of these materials consists of two-dimensional flat platelets (flakes), laid parallel to each other.

2. Fibrous Composites:

Fibrous composites consist of a matrix reinforced by a dispersed phase in form of fibers

- i. Short-fiber reinforced composites. Short-fiber reinforced composites consist of a matrix reinforced by a dispersed phase in form of discontinuous fibers.
- ii. Long-fiber reinforced composites. Long-fiber reinforced composites consist of a matrix reinforced by a dispersed phase in form of continuous fibers.

### 3. Laminate Composites:

When a fiber reinforced composite consists of several layers with different fiber orientations, it is called multilayer (angle-ply) composite.

## **1.7 PROCESSING**

### **1.7.1 Liquid State Processing**

Liquid state fabrication of Metal Matrix Composites involves incorporation of dispersed phase into a molten matrix metal, followed by its Solidification. In order to provide high level of mechanical properties of the composite, good interfacial bonding (wetting) between the dispersed phase and the liquid matrix should be obtained.

Wetting improvement may be achieved by coating the dispersed phase particles (fibers). Proper coating not only reduces interfacial energy, but also prevents chemical interaction between the dispersed phase and the matrix.

The methods of liquid state fabrication of Metal Matrix Composites are:

#### **1.7.1.1 Stir Casting**

Stir Casting is a liquid state method of composite materials fabrication, in which a dispersed phase (ceramic particles, short fibers) is mixed with a molten matrix metal by means of mechanical stirring [fig. 1.1]. Stir Casting is the simplest and the most cost effective method of liquid state fabrication. The liquid composite material is then cast by conventional casting methods and may also be processed by conventional Metal forming technologies. In this process particles are often tend to form agglomerates, which can be only dissolved by intense stirring [2]. However, here gas access into the melt must be absolutely avoided, since this could lead to unwanted porosities or reactions. Careful

attention must be paid to the dispersion of the reinforcement components, so that the reactivity of the components used is coordinated with the temperature of the melt and the duration of stirring, since reactions with the melt can lead to the dissolution of the reinforcement components. Because of the lower surface to volume ratio of spherical particles, reactivity is usually less critical with stirred particle reinforcement than with fibers.

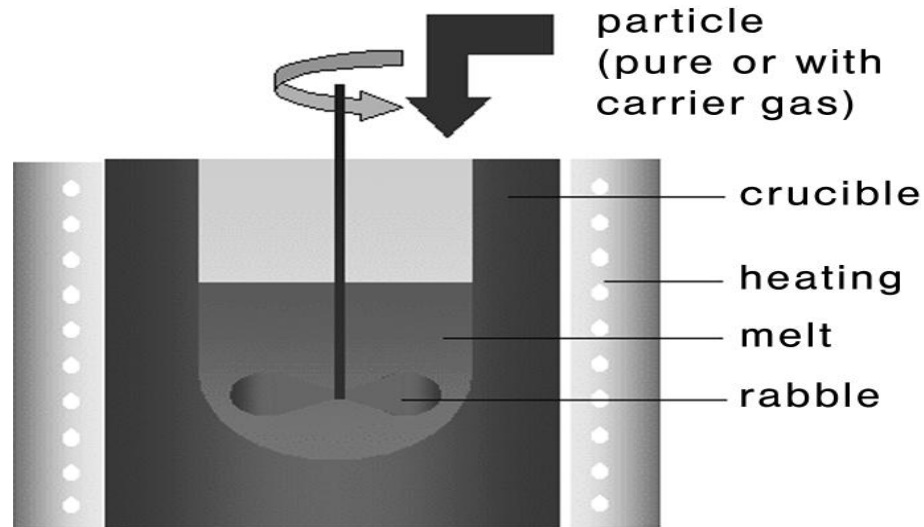


**Figure 1.1:** Stir casting [2]

Stir Casting is characterized by the following features:

1. Contents of dispersed phase are limited (usually not more than 30% by volume).
2. Distribution of dispersed phase throughout the matrix is not perfectly homogeneous:
  - i. There are local clouds (clusters) of the dispersed particles (fibers).
  - ii. There may be gravity segregation of the dispersed phase due to a difference in the densities of the dispersed and matrix phase
3. The technology is relatively simple and low cost

Distribution of dispersed phase may be improved if the matrix is in semi-solid condition. The method using stirring metal composite materials in semi-solid state is called

Rheocasting. High viscosity of the semi-solid matrix material enables better mixing of the dispersed phase.

### **1.7.1.2 Infiltration**

Infiltration is a liquid state method of composite materials fabrication, in which a preformed dispersed phase (ceramic particles, fibers, woven) is soaked in a molten matrix metal, which fills the space between the dispersed phase inclusions. The motive force of an infiltration process may be either capillary force of the dispersed phase (spontaneous infiltration) or an external pressure (gaseous, mechanical, electromagnetic, centrifugal or ultrasonic) applied to the liquid matrix phase (forced infiltration). Infiltration is one of the methods of preparation of tungsten-copper composites.

The principal steps of the technology are as follows:

- i. Tungsten Powder preparation with average particle size of about 1-5microns.
- ii. Optional step: Coating the powder with nickel. Total nickel content is about 0.04%.
- iii. Mixing the tungsten powder with a polymer binder.
- iv. Compacting the powder by a molding method (Metal injection molding, die pressing, isostatic pressing). Compaction should provide the predetermined porosity level (apparent density) of the tungsten structure.
- v. Solvent debinding
- vi. Sintering the green compact at 2200-2400F (1204-1315 °C) in Hydrogen atmosphere for 2 hours. Placing the sintered part on a copper plate (powder) in the infiltration/sintering furnace.
- vii. Infiltration of the sintered tungsten skeleton porous structure with copper at 2100-2300F (110-1260 °C) in either hydrogen atmosphere or vacuum for 1 hour.

### **1.7.1.3 Gas Pressure Filtration**

Gas Pressure Infiltration is a forced infiltration method of liquid phase fabrication of Metal Matrix Composites. It is using a pressurized gas for applying pressure on the molten metal and forcing it to penetrate into a preformed dispersed phase [fig. 1.2]. In gas

pressure infiltration the melt infiltrates the preform with a gas applied from the outside [2]. A gas that is inert with respect to the matrix is used. The melting of the matrix and the infiltration take place in a suitable pressure vessel.

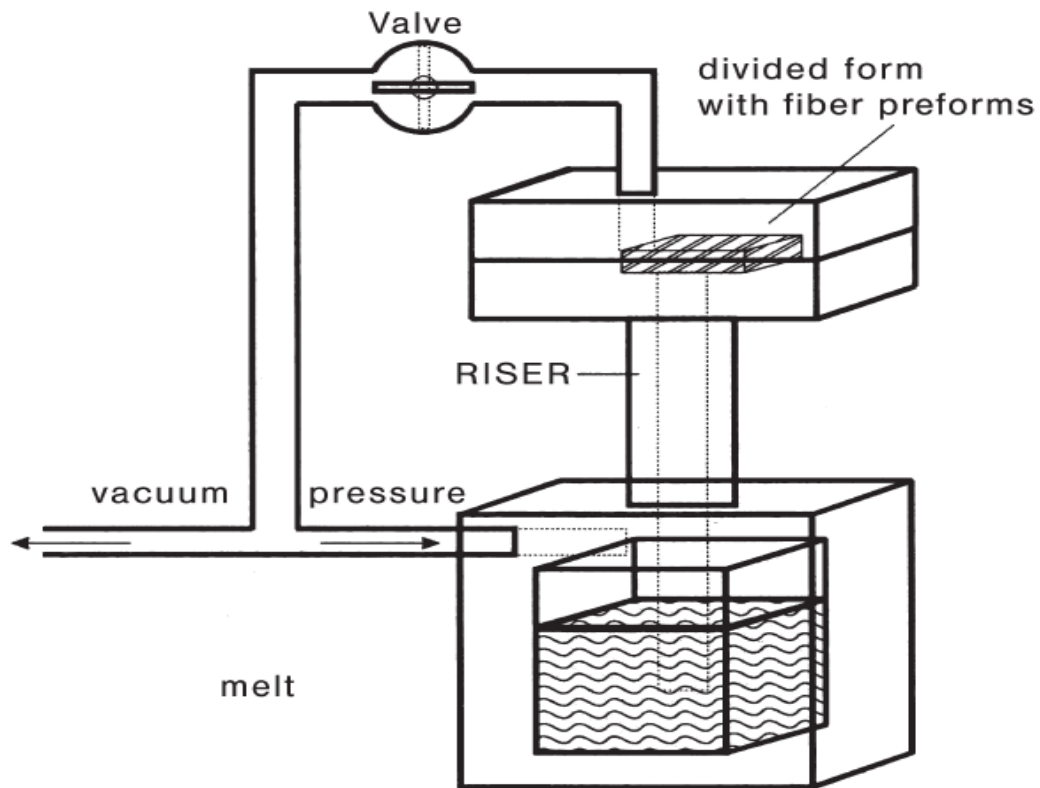


**Figure 1.2:** Gas Pressure Infiltration [2]

Gas Pressure Infiltration method is used for manufacturing large composite parts. The method allows using non-coated fibers due to short contact time of the fibers with the hot metal. In contrast to the methods using mechanical force, Gas Pressure Infiltration results in low damage of the fibers.

#### **1.7.1.4 Squeeze Casting Filtration**

Squeeze Casting Infiltration is a forced infiltration method of liquid phase fabrication of Metal Matrix Composites, using a movable mold part (ram) for applying pressure on the molten metal and forcing it to penetrate into a performed dispersed phase, placed into the lower fixed mold part [ fig1.3]. Squeeze Casting Infiltration method is similar to the

Squeeze casting technique used for metal alloys casting. Squeeze casting or pressure casting are the most common manufacturing variants for metal matrix composite [2]. After a slow mold filling the melt solidifies under very high pressure, which leads to a fine-grained structure. In comparison with die-casted parts the squeeze-casted parts do not contain gas inclusions, which permit thermal treatment of the produced parts.

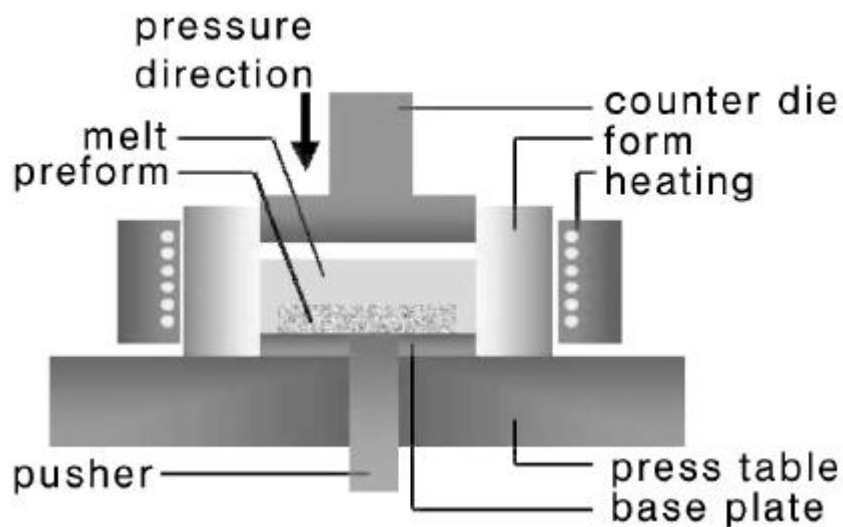


**Figure 1.3:** Squeeze Casting Infiltration [2]

Squeeze Casting Infiltration process has the following steps:

1. A preform of dispersed phase (particles, fibers) is placed into the lower fixed mold half.
2. A molten metal in a predetermined amount is poured into the lower mold half.
3. The upper movable mold half (ram) moves downwards and forces the liquid metal to infiltrate the preform.
4. The infiltrated material solidifies under the pressure.
5. The part is removed from the mold by means of the ejector pin.

The method is used for manufacturing simple small parts (automotive engine pistons from aluminium alloy reinforced by alumina short fibers).

### 1.7.1.5 Pressure Die Infiltration

Pressure Die Infiltration is a forced infiltration method of liquid phase fabrication of Metal Matrix Composites, using a die casting technology, when a preformed dispersed phase (particles, fibers) is placed into a die (mold) which is then filled with a molten metal entering the die through a sprue and penetrating into the preform under the pressure of a movable piston (plunger) [fig. 1.4].

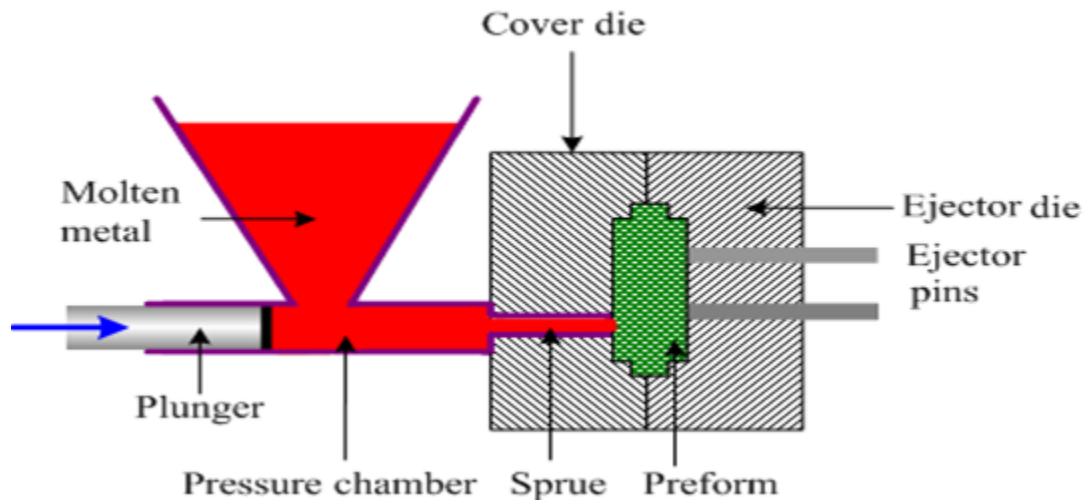


**Figure 1.4:** Pressure Die Infiltration [24]

### 1.7.2 Solid State Processing

Solid state fabrication of Metal Matrix Composites is the process, in which Metal Matrix Composites are formed as a result of bonding matrix metal and dispersed phase due to mutual diffusion occurring between them in solid states at elevated temperature and under pressure. Low temperature of solid state fabrication process (as compared to Liquid state fabrication of Metal Matrix Composites) depresses undesirable reactions on the boundary between the matrix and dispersed (reinforcing) phases.

Metal Matrix Composites may be deformed also after sintering operation by rolling, Forging, pressing, Drawing or Extrusion. The deformation operation may be either cold (below the recrystallization temperature) or hot (above the recrystallization temperature). Deformation of sintered composite materials with dispersed phase in form of short fibers

results in a preferred orientation of the fibers and anisotropy of the material properties (enhanced strength along the fibers orientation).

There are two principal groups of solid state fabrication of Metal Matrix Composites:

### 1.7.2.1 Diffusion Bonding:

Diffusion Bonding is a solid state fabrication method, in which a matrix in form of foils and a dispersed phase in form of long fibers are stacked in a particular order and then pressed at elevated temperature [3]. The finished laminate composite material has a multilayer structure. Diffusion Bonding is used for fabrication of simple shape parts (plates, tubes).

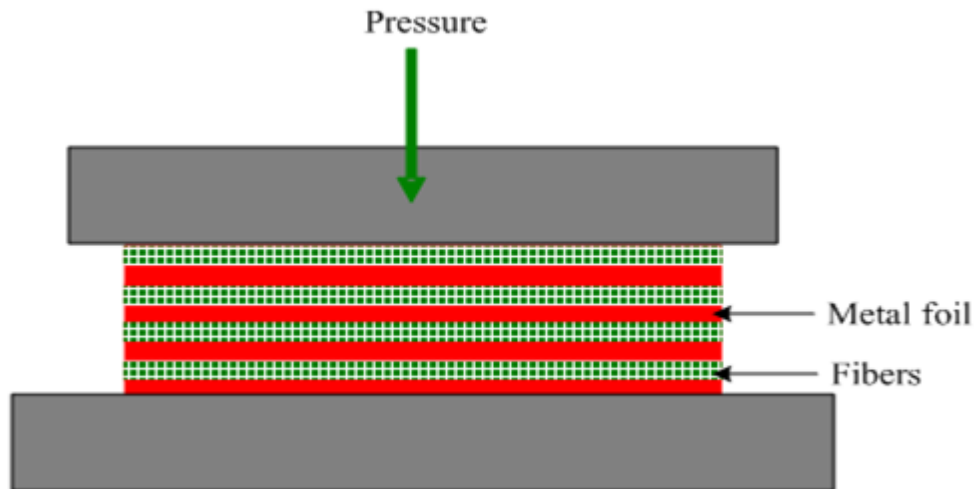


**Figure 1.5:** Diffusion Bonding [24]

Variants of diffusion bonding are roll bonding and wire/fiber winding. Roll Bonding is a process of combined rolling (hot or cold) strips of two different metals (e.g. steel and aluminium alloy) resulted in formation of a laminated composite material with a metallurgical bonding between the two layers. Wire/fiber Winding is a process of combined winding continuous ceramic fibers and metallic wires followed by pressing at elevated temperature.

### 1.7.2.2 Sintering:

Sintering fabrication of Metal Matrix Composites is a process, in which a powder of a matrix metal is mixed with a powder of dispersed phase in form of particles or short fibers for subsequent compacting and sintering in solid state (sometimes with some presence of liquid). Sintering is the method involving consolidation of powder grains by heating the “green” compact part to a high temperature below the melting point, when the material of the separate particles diffuse to the neighbouring powder particles. In contrast to the liquid state fabrication of Metal Matrix Composites, sintering method allows obtaining materials containing up to 50% of dispersed phase [3]. When sintering is combined with a deformation operation, the fabrication methods are called:

1. Hot pressing fabrication of metal matrix composite
2. Hot isostatic pressing fabrication of metal matrix composite
3. Hot powder extrusion pressing fabrication of metal matrix composite

#### 1. Hot Pressing Fabrication of Metal Matrix Composites:

In this fabrication process sintering under a unidirectional pressure applied by a hot press. The fabrication stages of hot pressing process is done in three stages.

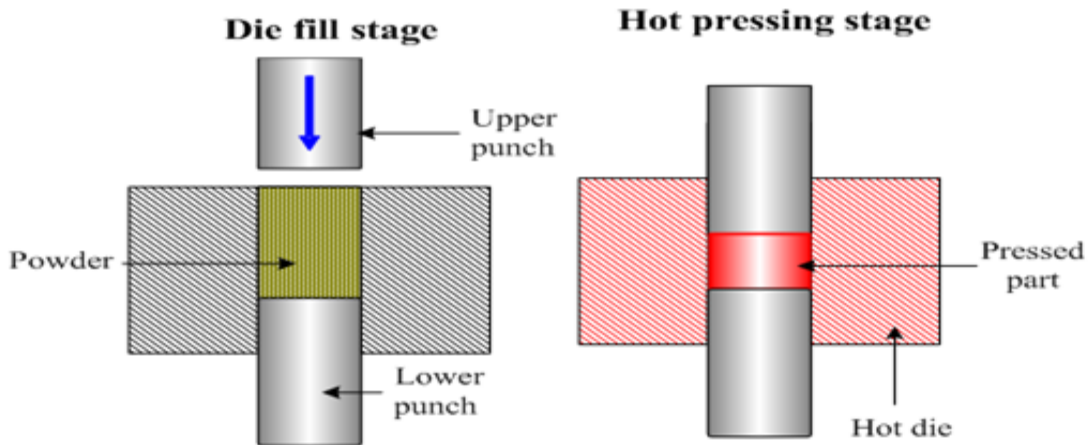


**Figure 1.6:** Die Fill stage [24]

**Figure 1.7:** Hot Pressing [24]

In the die fill stage [fig. 1.6], powder is put into the die and in second stage. There is hot pressing is to be done to pressed part in the die [fig. 1.7].

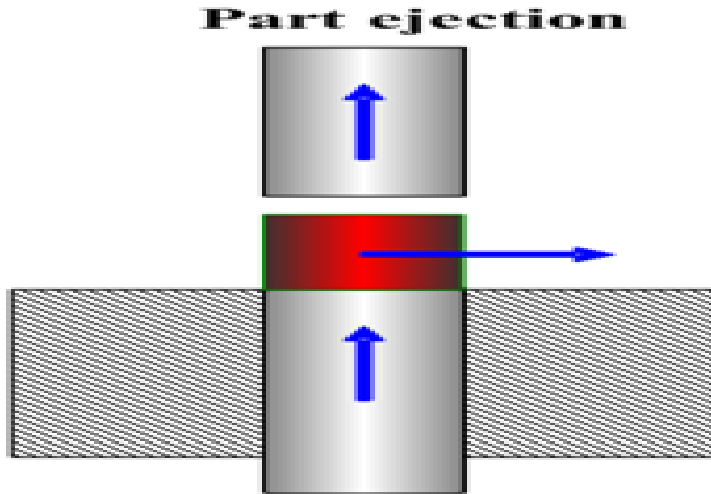


**Figure 1.8** Part Ejection [24]

In the last stage [fig 1.8], part is ejected, for this upper punch moves up to eject the part from the die.

2. Hot Isostatic Pressing Fabrication of Metal Matrix Composites:

In this process of fabrication sintering under a pressure applied from multiple directions through a liquid or gaseous medium surrounding the compacted part and at elevated temperature [fig. 1.9].

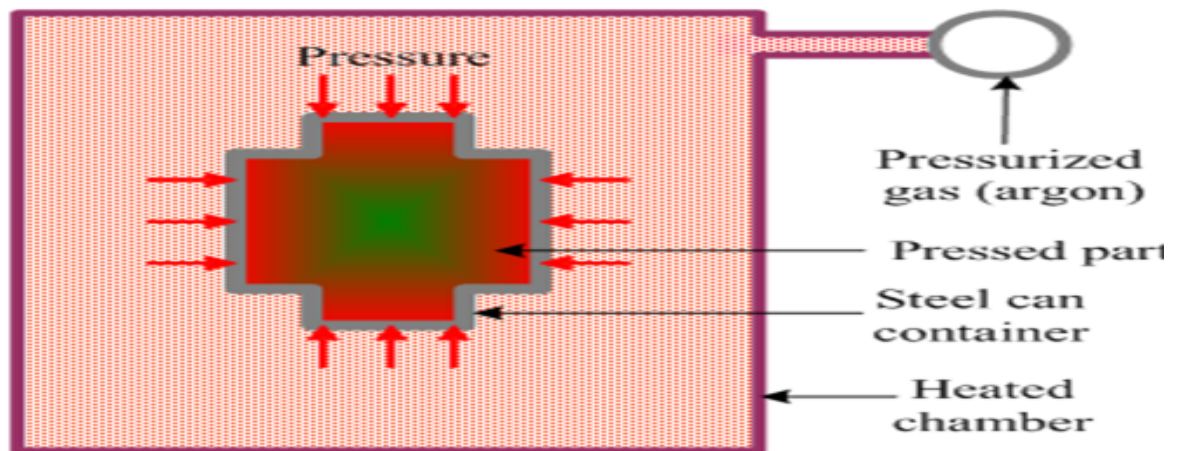


**Figure 1.9:** Hot Isostatic Pressing [24]

3. Hot Powder Extrusion Fabrication of Metal Matrix Composites:

In this process sintering is under a pressure applied by an extruder at elevated temperature. It is of two type, forward extrusion and backward extrusion [fig. 1.10].

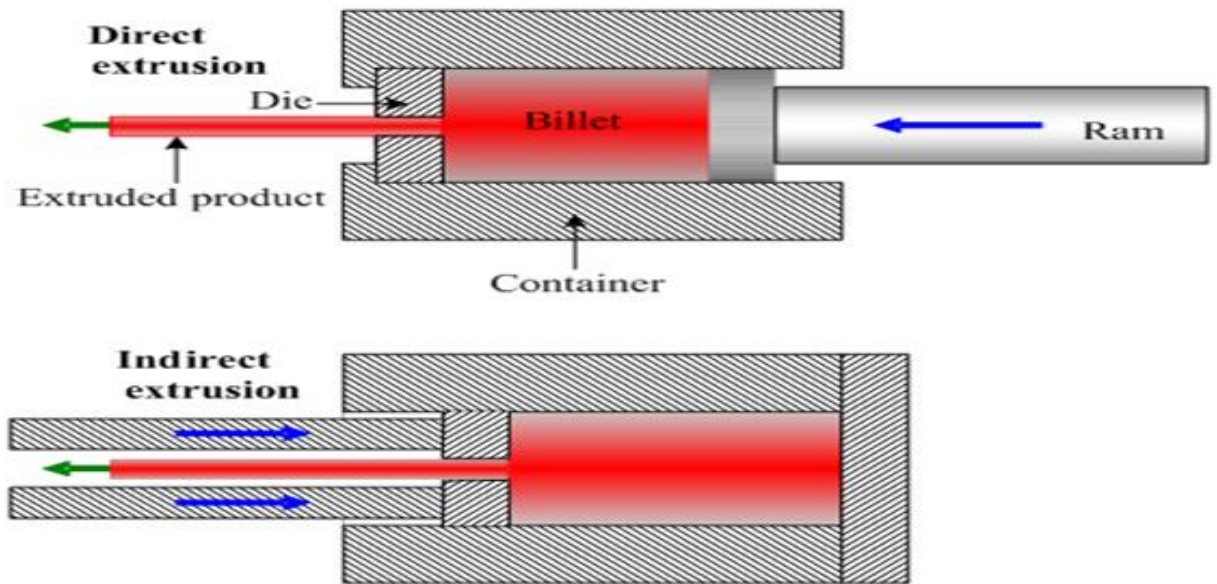


**Figure 1.10:** Extrusion [24]

## 1.8 APPLICATIONS

Applications of metal matrix composites can be conveniently grouped by market area, since each area requires set of properties and cost that result in particular subsets of metal matrix composite materials being of primary interest [3]. The primary markets for MMCs are divided into aerospace, automotive, commercial and industrial products, and electronics packaging which represents the area of greater interest.

1. Aerospace applications are the original driving force for metal matrix composite development. This is due to the quest for weight reduction for improved performance and payload capabilities combined with high value placed on weight savings. Examples for aerospace application are aircraft structure, aero engine, space structure and other space applications.
2. In the automotive market, properties of interest to the automotive engineer include increased stiffness, wear resistance, and improved cycle fatigue resistance. Weight saving is also important in automotive applications for achieving

performance improvements with much lower cost. Examples for automotive applications are engines, brake system, driveshaft and other automotive applications

3. In commercial and industrial sector, improved performance is highly valued. As a result many of materials that gain favour in aerospace industry market are also applied in this sector also. Examples for commercial and industrial sector are recreational, computer hard disk drives and other industrial applications.

## **1.9 THERMAL AGEING:**

Aluminium alloys which are heat treatable belong to systems with limited solubility in solid state. These are precipitation hardenable alloys. The main characteristics of this type of the alloy system is temperature-dependent equilibrium solid solubility, which increases with rise in temperature for greater hardness ageing is done and this is achieved by the phenomenon of precipitation [4]. If precipitation is done at room temperature with time is called natural ageing whereas precipitation at high temperature is referred to as artificial ageing, “age hardening” or just “ageing”. The maximum hardness and strength developed when alloy is aged at a suitable suitable temperature which normally ranges between 80 °C and 300 °C. Ageing time may vary from 4 hours to 24 hours.

The spontaneous decomposition of supersaturated solid solution takes place during ageing treatment. Higher the ageing temperature and higher the degree of super saturation more intensive will the ageing be. Besides mechanical properties, chemical properties are also effected by ageing. This happens due to the meta stable structure of alloy which are formed during ageing of supersaturated of solid solution obtained by solution treatment, rise in temperature changes the atomic position with corresponding change in the forces associated with inter atomic bonds. At the same time distribution of second phase particles also changes.

Following steps are associated with the process of precipitation hardening in most of aluminium alloys

1. The first stages preceding the formation of particles of the precipitating phase consists of rearrangement of atoms within the crystal lattice. This constitutes formation of clusters and Guinier-Preston zones (GP-I) during this process, mechanical properties are improved due to development of micro strains in the lattice
2. Formation of transition structure in the form of modified Guinier-Preston zones (GP-II) and intermediate this may give to maximum strengthening in the alloy.
3. Formation of stable phase from transition phases whose particles have common boundaries with the grain of the matrix.
4. Growth of the certain larger particles at the expense of neighbouring smaller particles. Due to this stress relief takes place in the lattice usually at higher ageing temperature, which causes considerable decrease in strength and increase in ductility of the alloy.

This chapter presents a review of the literature data available on the effect of various reinforcement types, their size and volume fraction, ageing behavior with Al based MMCs.

**A . Banerji et al** [5] had studied the abrasive wear rates of particulate composites of an Al-11.8Si-4Mg alloy containing of zircon particles (average size, 100  $\mu\text{m}$ ) were measured on an 80 grit aloxide cloth sheet as a function of the volume fraction of zircon, the applied load and the number of passes over the abrasive paper. When the volume fraction of zircon is above a critical value of 0.09, the abrasive wear resistance (reciprocal of the wear rate) increases with the volume fraction of zircon according to the rule of mixtures. When the volume fraction is fixed, the abrasive wear resistance increases with the number of passes possibly because of blunting of the alumina particles of the abrasive cloth. No improvement in the abrasive wear resistance of composites over the matrix alloy was observed when the volume fraction of zircon was below 0.09. Scanning electron microscopy studies of the abraded surfaces of composites revealed fractured zircon particles but no evidence of filler particle pull-outs or debonding at the interface was obtained.

**Sanjeev Das et al.** [6] had Synthesis and characterized of zircon sand/Al-4.5 wt%Cu composite produced by stir casting route. Coarser particles of size between 90 and 135  $\mu\text{m}$  can be dispersed in substantial amounts (up to 30 wt%), where as finer particles of size 15 and 65  $\mu\text{m}$  have limited dispersion, 10 and 20 wt%, respectively. The matrix of the composites has cellular structure, where the size of the cell depends on zircon particle size and its amount in the composite. Segregation of copper rich phase ( $\text{CuAl}_2$ ) has been found in the vicinity of the particle–matrix interface. The abrasive wear resistance of the composite improves with the increase in amount or decrease in size of zircon particles.

**Sanjeev Das et al.** [7] had studied ageing behavior of  $\text{Al}_2\text{O}_3$  and  $\text{ZrSiO}_4$  reinforced in Al–4.5 wt% Cu composite synthesized by stir casting route. Micro structural characterization

had been carried out to investigate the effect  $\text{Al}_2\text{O}_3$  and  $\text{ZrSiO}_4$  particulates on the microstructure of Al–4.5 wt% Cu matrix composite. It was found that  $\text{Al}_2\text{O}_3$  reinforced composite show high acceleration in age hardening compared to  $\text{ZrSiO}_4$  particulates, which is due to the breakage of  $\text{Al}_2\text{O}_3$  particles during melting and stirring process.

**Sanjeev Das et al.** [8] had studied the abrasive wear behavior of aluminium metal matrix composite reinforced with alumina and zircon sand particles has been carried out. Microstructures of the composites in as-cast condition show uniform distribution of particles and reveal better bonding in the case of zircon particles reinforced composite compared to that in alumina particles reinforced composite. Abrasive wear resistance of both the composites improves with the decrease in particle size. It was observed that the alumina particle reinforced composite shows relatively poor wear resistance property compared to zircon-reinforced composite.

**L. Pederson et al.** [9] had studied the effect of solution heat treatment and quenching rates on mechanical properties and microstructures in Al-Si-Mg foundry alloys. Four common Al-Si-Mg foundry alloys had been solution heat treated at 813 K, quenched, and immediately aged at 423 K for up to 240 minutes. The mechanical properties are found to be related to the amount of Mg and Si in the alloys. A high strength is obtained after only 60 minutes of solution heat treatment, indicating that the solid solution is rapidly saturated on Mg and Si. The ductility is very much related to the amount of silicon present and the refinement of the silicon crystals within the eutectic areas, since silicon crystals are observed to crack when load is applied. Thus, a well modified structure is the best way to obtain high ductility. Reduced quenching rates after solution heat treatment lead to a lower strength.

**Ashutosh Sharma et al.**[10] had investigated the age hardening behavior of Al–4.5%Cu alloy composite reinforced with zircon sand particulates and produced by stir casting route in different quenching media viz, water, oil, and salt brine solution (7 wt%). Optical microscopy of the as cast alloy composite indicates that the matrix of the composite has the cellular structure. The results of ageing demonstrate that the micro hardness of age hardenable Al–Cu based alloy composites depend on the quenching medium in which they are heat treated. Salt brine quenching is faster as compared to water and oil, even if higher

strength is obtained but cannot be used for complex shapes and thin sections where oil quenching is the alternative due to minimum distortion and cracking problems. Thermal cycling studies of the composite at 25–540 °C have been also carried out to determine the extent of quenching of the matrix after each solution heat treatment cycle while varying the quenching media.

**Lin Geng et al.** [11] had analyzed the age hardening behavior of the  $\text{Al}_2\text{O}_3/\text{Al-Cu}$  composites by measuring the hardness of the specimens at different aging temperatures and aging time. Microstructure of the composites was observed by transmission electron microscope (TEM). The results indicate that the hardness of the  $\text{Al}_2\text{O}_3/\text{Al-Cu}$  composites containing 7% Cu is much higher than that containing 1%-5% Cu because of the large amount of  $\text{CuAl}_2$  precipitant in the  $\text{Al}_2\text{O}_3/\text{Al-Cu}$  composite. With the increase of Cu content from 1% to 7%, the time needed for the appearance of peak hardness shortened, indicating that the addition of Cu can accelerate the kinetic of  $\text{CuAl}_2$  precipitation in the  $\text{Al}_2\text{O}_3/\text{Al-Cu}$  composites. The  $\text{Al}_2\text{O}_3/\text{Al-Cu}$  composite containing 7% Cu shows the highest increment of hardness by aging treatment.

**Y. Sahin et al.** [12] had presented that aluminium alloy composites containing various particle sizes of 10 and 20 wt.% SiC particles were prepared by molten metal mixing and squeeze casting method under argon gas. The stirring was carried out with graphite impeller during addition of particle. The molten mixture was poured into a die when the stirring was completed and metal matrix composites were produced by applying the pressure. Optical microscopic examination, hardness, density and porosity measurement were carried out. Moreover, metal matrix composites were machined at various cutting speeds under a fixed depth of cut and feed rate using different cutting tools. It is observed that there was a reasonably uniform dispersion of particles in the matrix alloy. The density decreased with decreasing particle sizes, but porosity decreased considerably with increasing particle size. In addition, the tool life decreased considerably with increasing cutting speeds for all tests.

**L.A. Dobrzanski et al.** [13] had studied the influence of temperature and time in the age-hardening on the selected mechanical properties and hardness of the  $\text{AlSi9Mg}$  alloy. The

efficiency of the age-hardening was tested on laboratory specimens through the statically tension test on ZWICK/Z100. Damages were critically assessed through SEM investigations. Evaluation the mechanical properties of prepared specimens were realized by solutionizing and then ageing in different periods of time. Adequately selected time of the ageing improved the hardening and plasticity and reduces the tendency of aluminium to formation of coagulations

**S.B. Hassan et al.** [14] had studied the microstructure and ageing behavior of Al–Si–Fe/Mg alloys produced through sand-casting route. 4.0–6.0 wt% Mg was added to Al–Si–Fe alloy. Standard mechanical properties test specimens were prepared from the sand cast 25 mm diameter by 45 mm rods. Thermal ageing was done for 6 h at 200 °C. The ageing characteristics of these alloys were evaluated using tensile properties, hardness values, impact energy and microstructure as criteria. The thermal aged specimens exhibited higher yield strength, tensile strength and hardness values as the weight percent of magnesium increased up to 5 wt% in the Al–Si–Fe/Mg alloys as compared to as-cast specimens. The optimum values were obtained at 5 wt% Mg. Lower percent elongation, reduction in area and impact energy values were obtained for age-hardened Al–Si–Fe/Mg alloy specimens as compared to as-cast specimens. The increases in hardness values and strength during ageing are attributed to the formation of coherent and uniform precipitation in the metal lattice. It was found that the age-hardened showed acceleration in ageing compared to the as-cast alloy. However, the 5 wt% Mg addition to the alloy showed more acceleration to thermal ageing treatment. These results show that better mechanical properties are achievable by subjecting the as-cast Al–Si–Fe/Mg alloys to thermal ageing treatment.

**M.M. Sharma et al.** [15] had compared the aging response of various Al–Zn–Mg–Cu alloys with the reinforced counterpart. The effects of aging temperature and time on the mechanical properties of these alloys, was also determined. Moreover, the effects of quenching rate from solution temperature, time between quench and aging, and heating rate to precipitation temperature were investigated. The study was executed by selecting two different heat treatments for each of three different aging temperatures: one without prior straining, and the other with 2% straining prior to aging to relieve stress. Room

temperature tensile testing was conducted to determine these variations of aging on the strength of the spray formed Al–Zn–Mg–Cu alloys. The presence of SiC particles accelerated the aging kinetics of the alloys compared to the unreinforced counterparts. This difference in time to peak aging decreased with decreasing aging temperature. At uniform temperatures, differences for time to peak aging between unreinforced and composite alloys also existed in both the prestrained and unstrained condition. The difference was not as great in the prestrained state. The tensile strengths increased slightly with prestraining, but not significantly. Alloys containing silver maintained high strengths over silver-free counterparts when rapidly heated to precipitation temperatures above 120 °C. At slow heating rates, however, the silver-free alloys matched or were slightly higher than the strength of silver alloys, with increasing heating rate.

**Sharmilee Pal et al.** [16] had studied the age-hardening kinetics of powder metallurgy processed Al–Cu–Mg alloy and composites with 5, 15 or 25 vol.% SiC reinforcements, subjected to solution treatment at 495 °C for 0.5 h or at 504 °C for 4 h followed by aging at 191 °C. The Al–SiC interfaces in composites show undissolved, coarse intermetallic precipitates rich in Cu, Fe, and Mg, with its extent varying with processing conditions. Examination of aging kinetics indicates that the peak-age hardness values are higher, and the time taken for peak aging is an hour longer on solutionizing at 504 °C for 4 h, due to greater solute dissolution. Contrary to the accepted view, the composites have taken longer time to peak-age than the alloy, probably due to lower vacancy concentration, large-scale interfacial segregation of alloying elements, and inadequate density of dislocations in matrix. The composite with 5 vol. % SiC with the lowest inter-particle spacing has shown the highest hardness.

**R.N. Rao et al.** [17] had investigated the effect of matrix alloy and influence of SiC particle on the sliding wear characteristics of high strength aluminium alloys AA7010, AA7009 and AA2024, composites was examined under varying applied pressure and a fixed sliding speed of 3.35 m/s. The results revealed that the wear resistance of the composite was noted to be significantly higher than that of the alloy and is suppressed further due to addition of SiC particles. The overall observation among the matrix alloys, AA7010 alloy shows maximum wear resistance than that of the other, and can withstand

the seizure pressure up to 2.6 MPa. The wear mechanism was studied through worn surfaces and microscopic examination of the developed wear tracks. The wear mechanism strongly dictated by the formation and stability of oxide layer, mechanically mixed layer (MML) and subsurface deformation and cracking. The overall results indicate that the high strength aluminium alloys and composite could be considered as an excellent material where high strength and wear resistance components are prime importance especially designing for structural applications in aerospace and general engineering sectors.

**Sharma Rajesh et al.** [18] had represents the influence of solutionizing temperature during artificial age hardening treatment (T6) of cast Al-(8,12,16%)Si-0.3%Mg on abrasive wear behavior. Alloys were prepared by controlled melting and casting. Cast alloys were given artificial age hardening treatment having a sequence of solutionizing, quenching and artificial aging. All the alloys were solutionized at 450 °C, 480 °C, 510 °C, and 550 °C for 8 h followed by water quenching (30 °C) and aging hardening at 170 °C for 12 h. Abrasive wear tests were conducted against 320 grade SiC polishing papers at 5 N and 10 N normal loads. It was observed that the silicon content and solution temperature affected the wear resistance significantly. Increase in solution temperature improved the wear resistance. Hypereutectic alloy showed better wear resistance than the eutectic and hypoeutectic alloys under identical conditions. Optical microstructure study of alloys revealed that the increase in solutionizing temperature improved distribution of silicon grains. Scanning electron microscopy (SEM) of wear surface was carried out to analyze the wear mechanism.

**T. V. S. Reddy et al** [19] had studied the effect of stir casting on the microstructure and adhesive wear characteristics of cast Al–Si–Cu alloy. They described the microstructure, hardness, and wear characteristics of cast aluminium-silicon alloy produced by a stir-casting technique. A hypoeutectic (Al-7% Si-0.8% Cu) alloy was cast under different stirring speeds. The stirring of semi-solid metal (SSM) slurries was performed under continuous cooling conditions from liquidus temperature. Wear characteristics of the alloys under investigation were studied using a pin-on-flat wear system over a range of normal loads (10-40N) at constant average sliding speed (0.2 m/s) against cast iron and

stainless steel counter surfaces. Stir-casting resulted in a material with higher micro hardness and lower wear rates than conventional cast alloy. Both the stir-cast and conventional cast alloy showed higher weight loss against the stainless steel compared with that against the cast iron counter surface. Optical microscopy of the conventional cast and stir-cast alloys showed that the stir-casting results in spheroidization and refinement of primary alpha aluminium and modification of eutectic silicon. The scanning electron microscopy of wear surfaces was carried out to investigate the mode of wear.

**Manchang Gui et al** [20] had studied the microstructure and mechanical properties of the composites and the unreinforced alloys in as-cast and heat treatment conditions are analyzed and evaluated. In 15 vol.% SiCp reinforced Mg-Al9Zn alloy-based composite (Mg-Al9Zn/15SiCp), SiC particles distribute homogenously in the matrix and are well bonded with magnesium. In 15 vol.% SiCp reinforced Mg-Zn5Zr alloy-based composite (Mg-Zn5Zr/15SiCp), some agglomerations of SiC particles can be seen in the microstructure. In the same stirring process conditions, SiC reinforcement is more easily wetted by magnesium in the Mg-Al9Zn melt than in the Mg-Zn5Zr melt. The significant improvement in yield strength and elastic modulus for two composites has been achieved, especially for the Mg-Al9Zn/15SiCp composite in which yield strength and elastic modulus increase 112 and 33%, respectively, over the unreinforced alloy, and increase 24 and 21%, respectively, for the Mg-Zn5Zr/15SiCp composite. The strain-hardening behaviors of the two composites and their matrix alloys were analyzed based on the microstructure characteristics of the materials.

**Peng Yu et al.** [21] had studied Precipitation hardening by further aging the alumina reinforced Al-Cu alloy matrix composite at 250° C . In situ formed micron-sized alumina particles were present in the Al(Cu) matrix of the un-aged composite, while additional nanometer-sized Al<sub>2</sub>Cu rods were obtained in the matrix of the aged composite. Both hardness and bending strength were enhanced after the composite was aged

**Yahya Altunpak et al** [22] had investigated with various aging heat treatment and machinability parameters in an aluminium-silicon based (LM-13) MMCs, produced by infiltration method. The composites had been subjected to heat treatment at different temperatures and times. In the milling of alumina short fiber reinforced LM-13

aluminium alloys, the surface integrity decreased when feed rate increased. It was found that increasing amount of fiber reinforcement and solutionizing temperature had significant effect on the surface integrity and sub-surface damage of the materials. Increasing the solutionizing temperature and fiber reinforcement produced higher  $R_a$  and  $R_{max}$  values. Microhardness measurement indicated that the sub-surface damage and the hardness increased by increasing the feed rate and fiber content.

It was observed from the review of available literature following gaps are identified

1. Work should be done to produce high quality and low cost reinforcement from industrial waste and by-products.
2. Efforts should be made on the development of AMCs based on non-standard aluminium alloys as matrix.
3. Work should be done to develop re-cycling technology for AMCs.
4. Work must be done for to develop simple and affordable joining techniques for AMCs.

Out of these gaps it was decided to work on aluminium alloy LM4 as matrix and zircon sand as reinforcement for synthesis of composite by stir casting route.

The problem is basically to study the effect of thermal ageing on aluminium alloy metal matrix composite (MMC) made by stir /sand casting technique. The change in mechanical properties would also be taken into consideration.

For the achievement of the above objective, an experimental set up was designed and prepared. The aim of the experiment was to study the effect of parameters, ageing temperature, ageing time and to observe the rate of change of mechanical properties of the metal matrix composites (MMC). The specimen is to be held in experimentation for pre-decided time periods and then change in the properties will be analyzed. The natural ageing of Aluminium alloy metal matrix composites will take long time so accelerated thermal ageing method is selected.

#### 4.1 Synthesis of Aluminium alloy/zircon sand composite

The raw material which is used in the synthesis of composite is as follows:

##### 4.1.1 Matrix Material

Aluminium alloy is used as matrix in the synthesis of composite. Chemical composition of used alloy is given in table 4.1

**Table 4.1 Chemical composition of aluminium alloy LM4**

Element	Al	Si	Cu	Fe	Ti	Mg
Wt%	89.7	4.95	3.1	0.722	0.165	0.113

##### 4.1.2 Reinforcement Material

Zircon sand was used as the reinforcement material. Particle size of zircon sand was in the range between 85-150  $\mu\text{m}$ . Particle size of reinforcement material is given table 4.2

**Table 4.2 Particle size of reinforcement material**

Reinforcement	Particle Size Range
Zircon Sand	85-150 $\mu\text{m}$

Chemical composition of reinforcement material is given in table 4.3

**Table 4.3 Chemical Composition of reinforcement material**

<b>Components</b>	<b>ZrO<sub>2</sub></b>	<b>SiO<sub>2</sub></b>	<b>TiO<sub>2</sub></b>	<b>Fe<sub>2</sub>O<sub>3</sub></b>	<b>Volatile</b>
<b>Wt %</b>	65.30	32.80	0.27	0.12	1.51

## **4.2 Synthesis**

A stir casting set up [fig 4.2] was fabricated which consisted of muffle furnace and stirrer assembly to synthesize the composite. The stirrer assembly which was used consisted of stirrer of graphite which connects with motor with speed (22-840 rpm). Crucible [fig 4.3] used for synthesis is of capacity of 1.5 Kg. The aluminium alloy is melted in crucible at 815° C. For reinforcement zircon sand was preheated at temperature 450° C to remove moisture from the particulate. The stirrer speed was 580 rpm to create vortex into the molten form and the preheated zircon particle was added at the rate of 10gm/min into the melt. After addition of preheated Zircon particle into the melt, stirring was done for 5-10 min for better distribution of zircon particle. Metal mould [fig 4.4] was used for pouring the melt.

The parameters which are important in the synthesis of composite are stirrer design, preheating temperature for particulate and stirring speed. These parameters are discussed below.

### **4.2.1 Stirrer Design**

It is very important parameter for stir casting process. It essentially requires for vortex formation for the uniform dispersion of particulate. There is a no uniform dispersion of particulate in case of no vortex formation.

#### **4.2.2 Particle Preheating Temperature**

Preheating of particulate is necessary to avoid moisture from the particulate otherwise there is chance of agglomeration of particulate due moisture and gases. Preheating of particulate is done on temperature of 450° C.

#### **4.2.3 Stirring Speed**

In stir casting process stirring is very important parameter for consideration. In the process stirring speed was 580 rpm which was effectively producing vortex without any spattering. It is also found that at less speed, dispersion of particulates are not proper because of uneffective vortex.

#### **4.3 Thermal Ageing**

The following steps which were followed in this heat treatment are as follows:

1. Solution heat treatment: Specimen is heated at temperature 535 °C for 1 hour.
2. Quenching: After that specimens are quenched in water and brine solution.
3. Ageing: Ageing is done at temperature 170 °C and 190 °C for 2 hours.

#### **4.4 Quenching Media**

The quenching media which are used after solution treatment are as follows:

1. Water
2. Brine Solution

## 4.5 Experiment plan

The experiment plan [fig 4.1] which is used during work is as follows

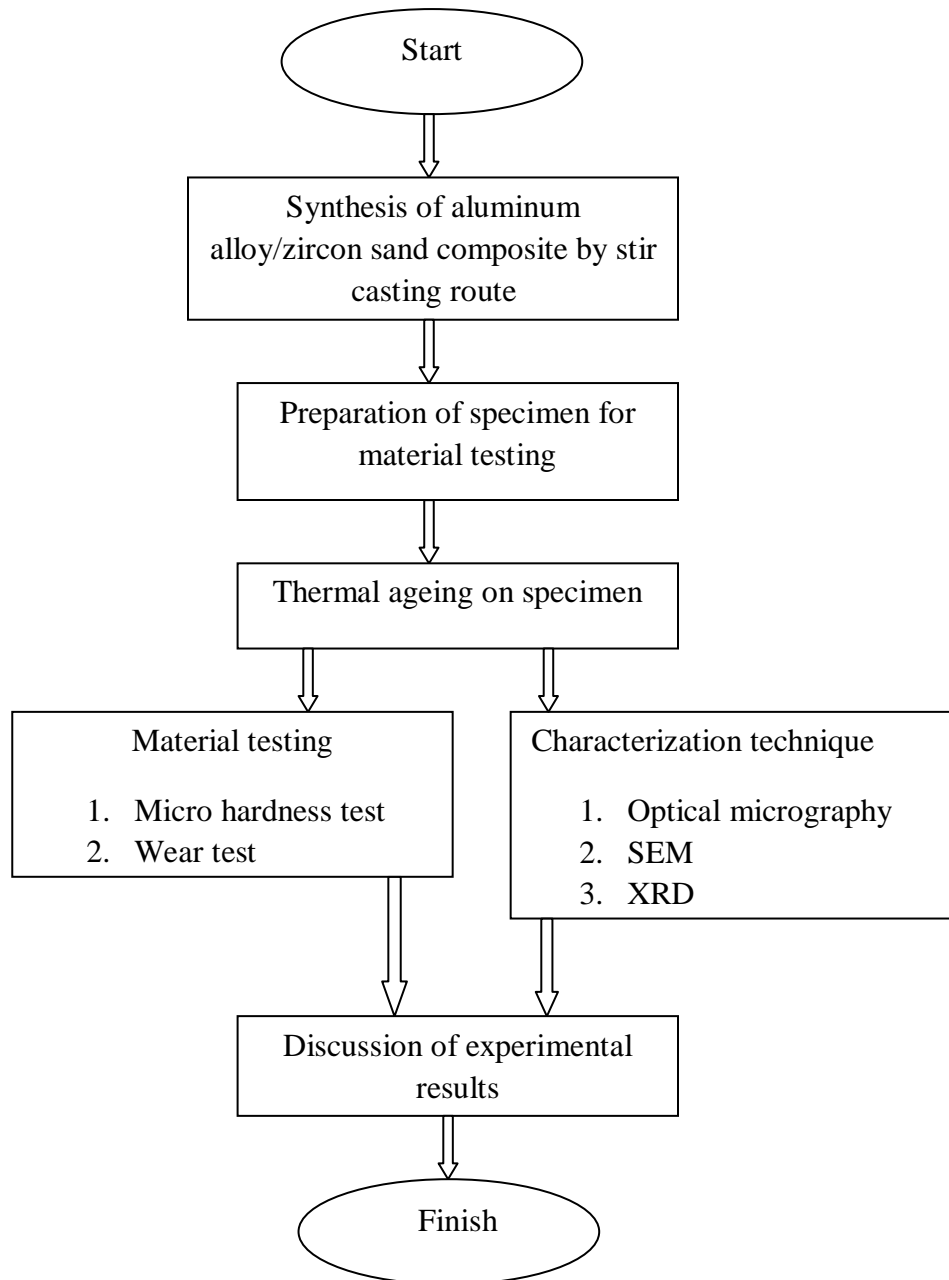


**Figure 4.1:** Work Plan

#### 4.6 Parameter Matrix

On the basis of type of material, ageing temperature and quenching media the parameter matrix is as follows

**Table 4.4 Parameter Matrix**

Specimen	Type	Quenching Media	Ageing Temperature
1	C1	W	170
2	C1	W	190
3	C1	B	170
4	C1	B	190
5	C2	W	170
6	C2	W	190
7	C2	B	170
8	C2	B	190

C1= Aluminium alloy

C2=Aluminium alloy10 wt% zircon sand

T1 = 170 °C

T2 = 190 °C

W = Water

B = Brine Solution

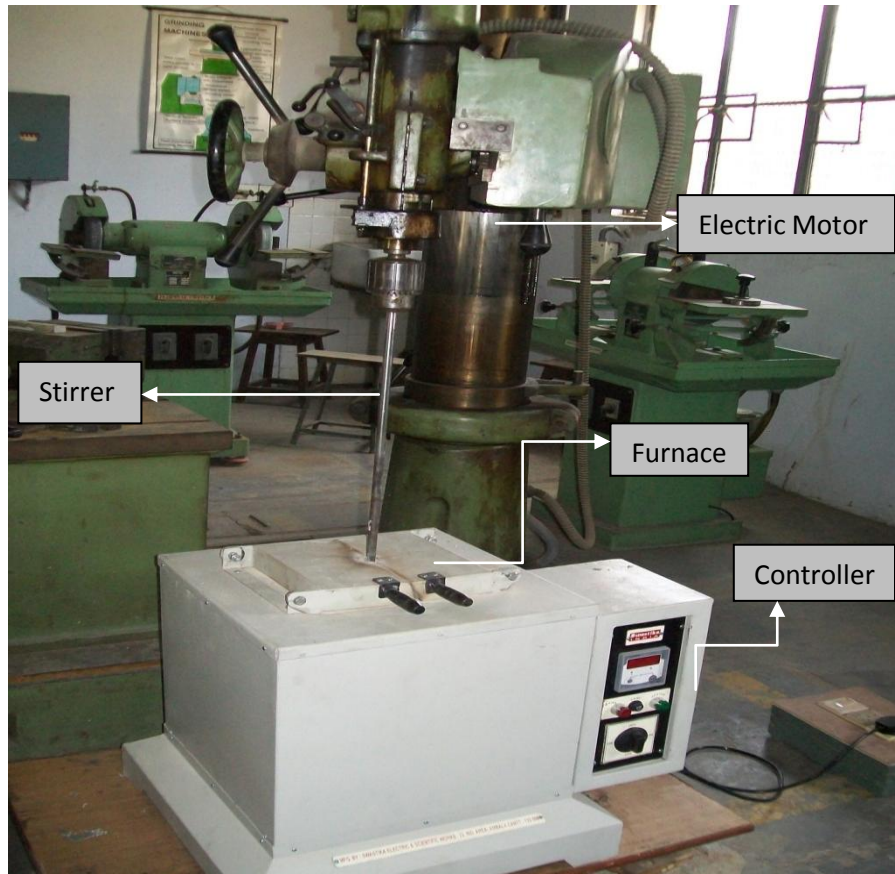


**Figure 4.2** Stir casting set up



**Figure 4.3** Crucible



**Figure 4.4** Metal mould

## 4.7 Material Characterization

Micro hardness is measured with the help of micro hardness tester .Wear rate is calculate with the help of weight loss technique.

### 4.7.1 Micro hardness tester

Micro hardness testing is a method for measuring the hardness of a material on a microscopic scale. A precision diamond indenter is impressed into the material at loads from a few grams to 1 kilogram. The impression length, measured microscopically, and the test load are used to calculate a hardness value.

The indentations are typically made using either a square-based pyramid indenter (Vickers hardness scale) or an elongated, rhombohedral-shaped indenter. The tester applies the selected test load using dead weights. The length of the hardness impressions are precisely measured with a light microscope using either a filar eyepiece or a video image and computer software. A hardness number is then calculated using the test load, the impression length, and a shape factor for the indenter type used for the test.



**Figure 4.5** Microhardness Tester

### 4.7.2 Wear testing machine

Wear rate testing is a method for measuring the wear loss of a material on a weight loss technique.



**Figure 4.6** Wear testing machine

## 4.8 Characterization Technique

Particles distribution was evaluated with the help of optical microscope .XRD studies were carried out to confirm the presence of reinforcement in the alloy matrix. Scanning electron microscopy of the specimens was studied.

### 4.8.1 X-ray diffraction

X-ray powder diffraction (XRD) is a rapid analytical technique primarily used for phase Identification of crystalline material and can provide information on unit cell dimensions. It is a versatile, non-destructive technique that reveals detailed information about the chemical composition and crystallographic structure of natural and manufactured materials. By varying the angle theta, the Bragg's Law conditions are satisfied by different d-spacing in polycrystalline materials.

$$n\lambda=2d\sin\theta$$

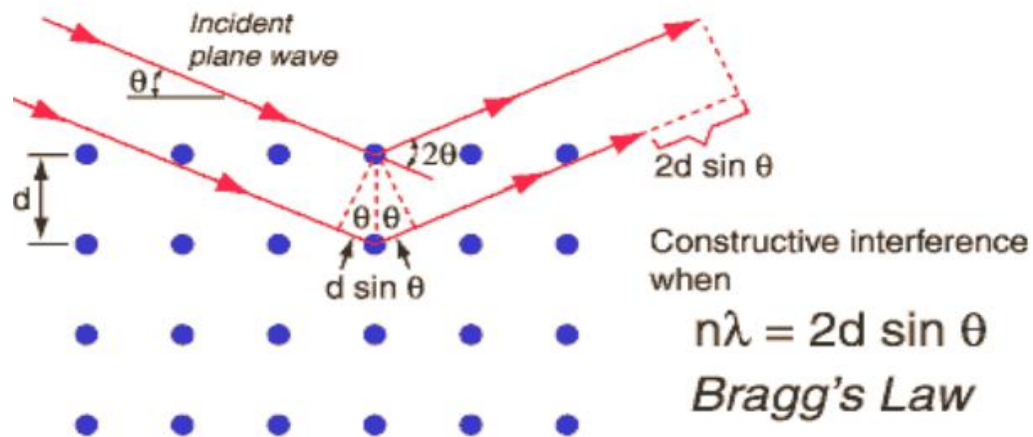


**Figure 4.7** Schematic for Bragg's law.

Max von Laue, in 1912, discovered that crystalline substances act as three-dimensional diffraction gratings for X-ray wavelengths similar to the spacing of planes in a crystal lattice. X-ray diffraction is now a common technique for the study of crystal structures and atomic spacing.

X-ray diffraction is based on constructive interference of monochromatic X-rays and a crystalline specimen. These X-rays are generated by a cathode ray tube, filtered to produce monochromatic radiation, collimated to concentrate, and directed toward the specimen. The interaction of the incident rays with the specimen produces constructive interference (and a diffracted ray) when conditions satisfy Bragg's Law. This law relates the wavelength of electromagnetic radiation to the diffraction angle and the lattice spacing in a crystalline specimen. These diffracted X-rays are then detected, processed and counted. A detector records and processes this X-ray signal and converts the signal to a count rate which is then output to a device such as a printer or computer monitor.

The geometry of X-ray diffractometer is such that the specimen rotates in the path of the collimated X-ray beam at an angle  $\theta$  while the X-ray detector is mounted on an arm to collect the diffracted X-rays and rotates at an angle of  $2\theta$ . The instrument used to maintain the angle and rotate the specimen is termed a goniometer. By scanning the specimen through a range of  $2\theta$  angles, all possible diffraction directions of the lattice should be attained due to the random orientation of the powdered material. Conversion of the diffraction peaks to d-spacing allows identification of the mineral because each

mineral 25 has a set of unique d-spacing. Typically, this is achieved by comparison of d-spacing with standard reference patterns.

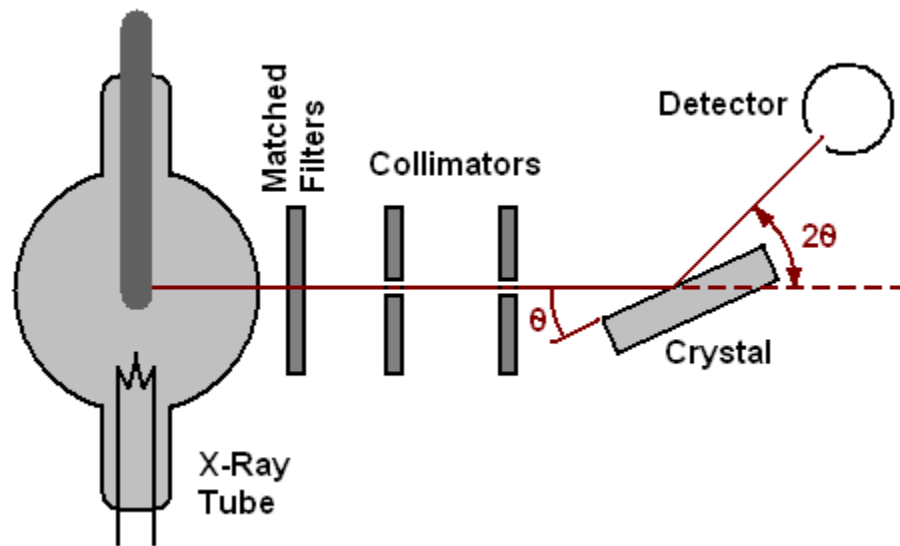


**Figure 4.8** Experimental set-ups for X-ray diffractometer

All diffraction methods are based on generation of X-rays in an X-ray tube. These X-rays are directed at the specimen, and the diffracted rays are collected. A key component of all diffraction is the angle between the incident and diffracted rays. For typical powder patterns, data is collected at  $2\theta$  from  $\sim 5^\circ$  to  $70^\circ$ , angles that are preset in the X-ray scan

#### **4.8.2 Scanning Electron Microscope**

The scanning electron microscope (SEM) is a type of electron microscope that images the specimen surface by scanning it with a high-energy beam of electrons in a raster scan pattern. The SEM is a microscope that uses electrons instead of light to form an image. The electrons interact with the atoms that make up the specimen producing signals that contain information about the specimen's surface topography, composition and other properties such as electrical conductivity. The scanning electron microscope has many advantages over traditional microscopes. The SEM has a large depth of field, which allows more of a specimen to be in focus at one time. The SEM also has much higher resolution ( $\sim 1$  nm), so closely spaced specimens can be magnified at much higher levels. Because the SEM uses electromagnets rather than lenses, the researcher has much more control in the degree of magnification. All of these advantages, as well as the actual

strikingly clear images, make the scanning electron microscope one of the most useful instrument in research today.

In a typical SEM, as shown in Figure 4.9, an electron beam is thermionically emitted from an electron gun fitted with a tungsten filament cathode. Tungsten is normally used in thermionic electron guns because it has the highest melting point and lowest vapour pressure of all metals. The electron beam, which typically has an energy ranging from a few hundred eV to 40 keV, is produced at the top of the microscope by an electron gun. The electron beam follows a vertical path through the microscope, which is held within a vacuum. The beam passes through pairs of scanning coils or pairs of deflector plates in the electron column, typically in the final lens, which deflect the beam in the  $x$  and  $y$  axes so that it scans in a raster fashion over a rectangular area of the specimen surface. Once the beam hits the specimen, electrons and X-rays are ejected from the specimen. Detectors collect these X-rays, backscattered electrons, and secondary electrons and convert them into a signal that is sent to a screen similar to a television screen. This produces the final image.

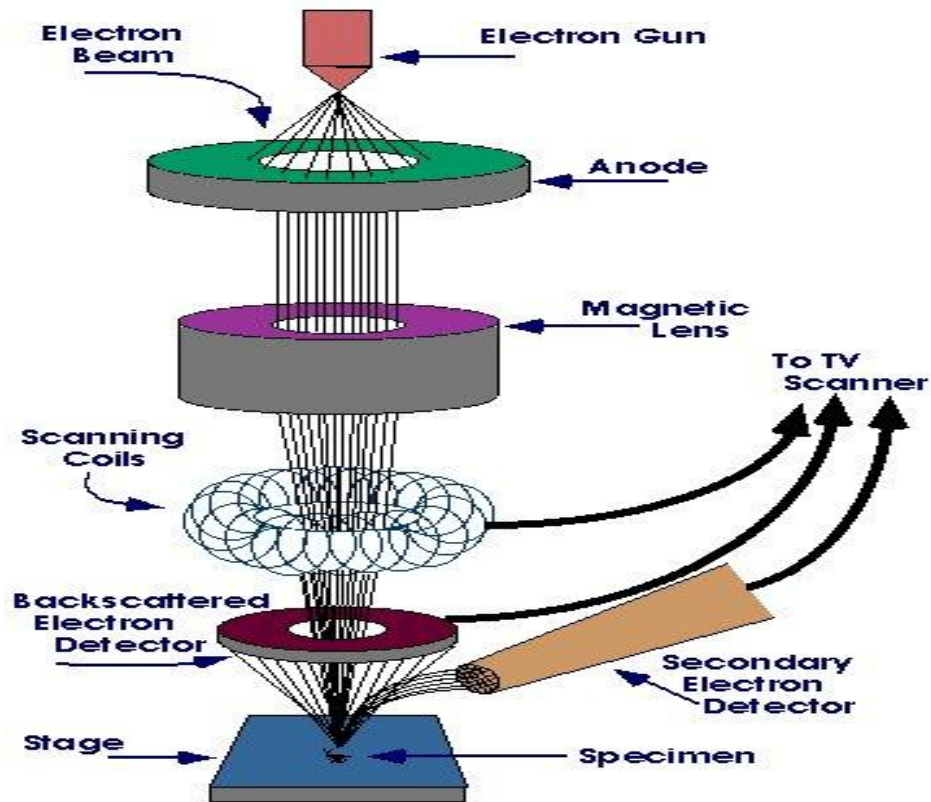


**Figure 4.9** Experimental set-up for scanning electron microscope (SEM)

All specimens must also be of an appropriate size to fit in the specimen chamber and are generally mounted rigidly on a specimen holder called a specimen stub. Several models of SEM can examine any part of a 6-inch (15 cm) semiconductor wafer, and some can tilt an object of that size to 45 degrees. For conventional imaging in the SEM, specimens must be electrically conductive, at least at the surface, and electrically grounded to prevent the accumulation of electrostatic charge at the surface. Metal objects require little special preparation for SEM except for cleaning and mounting on a specimen stub. Nonconductive specimens tend to charge when scanned by the electron beam, and especially in secondary electron imaging mode, this causes scanning faults and other image artifacts. They are therefore usually coated with an ultra-thin coating of electrically-conducting material, commonly gold, deposited on the specimen either by low vacuum sputter coating or by high vacuum evaporation. Conductive materials in current use for specimen coating include gold, gold/palladium alloy, platinum, osmium, iridium, tungsten, chromium and graphite. Coating prevents the accumulation of static electric charge on the specimen during electron irradiation.

Two important reasons for coating, even when there is more than enough specimen conductivity to prevent charging, are to maximize signal and improve spatial resolution, especially with specimens of low atomic number ( $Z$ ). Broadly, signal increases with atomic number, especially for backscattered electron imaging. The improvement in resolution arises because in low- $Z$  materials such as carbon, the electron beam can penetrate several micrometers below the surface, generating signals from an interaction volume much larger than the beam diameter and reducing spatial resolution. Coating with a high- $Z$  material such as gold maximizes secondary electron yield from within a surface layer a few nm thick, and suppresses secondary electrons generated at greater depths, so that the signal is predominantly derived from locations closer to the beam and closer to the specimen surface than would be the case in an uncoated, low- $Z$  material.

## Results and Discussions

---

### 5.1 Micro Hardness Test

A micro hardness tester MVH-1 is used for the micro hardness measurement. The specimens are grinded from top and bottom side for appropriate measurement. The load applied is of 200 gm at dwell time of 20 second.

**Table 5.1 Micro hardness data of alloy after ageing of 2 hours**

Specimen no.	Trial 1	Trial 2	Trial 3	Trial 4	Average
Specimen 1	52.7474	47.4242	45.9760	46.7375	48.1508
Specimen 2	44.8524	45.9760	44.2765	43.0692	44.5062
Specimen 3	50.0428	45.223	45.968	48.3537	47.3036
Specimen 4	45.007	44.8524	44.8524	43.9045	44.6540

The table 5.1 consist of value of micro hardness measurement of alloy after solution treatment at 535°C and then quenched in water and brine solution. After quenching the specimens, ageing is done at 170°C and 190°C for 2 hours.

**Table 5.2 Micro hardness data of composite after ageing of 2 hours**

Specimen no.	Trial 1	Trial 2	Trial 3	Trial 4	Average
Specimen 5	46.3515	45.3856	49.6123	46.822	47.5427
Specimen 6	48.537	45.9760	44.4870	44.12611	45.7356
Specimen 7	52.747	52.2816	51.3684	47.9448	51.085
Specimen 8	59.9792	60.5535	56.7415	54.181	57.8731

The table 5.2 consist of value of micro hardness measurement of composite after solution treatment at 535°C and then quenched in water and brine solution. After quenching the specimens, ageing is done at 170°C and 190°C for 2 hours.

**Table 5.3 Micro hardness data of alloy after ageing of 4 hours**

Specimen no.	Trial 1	Trial 2	Trial 3	Trial 4	Average
Specimen 1	35.0548	40.1168	36.9246	37.1788	37.3118
Specimen 2	36.093	36.9029	37.2453	36.3602	36.6503
Specimen 3	34.0545	41.0663	40.1224	41.39285	39.1590
Specimen 4	40.22375	40.7461	41.0215	40.1165	40.5269

The table 5.3 consist of value of micro hardness measurement of alloy after ageing of 4 hours at 170°C and 190° C.

**Table 5.4 Micro hardness data of composite after ageing of 4 hours**

Specimen no.	Trial 1	Trial 2	Trial 3	Trial 4	Average
Specimen 5	45.976	46.7487	46.8245	44.8521	46.1003
Specimen 6	46.7455	48.353	49.5426	49.6235	48.5661
Specimen 7	42.4579	47.9118	43.8652	45.5965	44.9578
Specimen 8	56.713	60.06	57.8267	51.822	56.198

The table 5.4 consist of value of micro hardness measurement of composites after ageing of 4 hours at 170°C and 190° C.

**Table 5.5 Micro hardness data of alloy after ageing of 8 hours**

Specimen no.	Trial 1	Trial 2	Trial 3	Trial 4	Average
Specimen 1	32.2061	38.0254	38.9012	30.6461	34.9447
Specimen 2	36.8707	36.1232	35.2014	33.7487	35.4860
Specimen 3	35.3102	36.9029	35.5684	37.7400	36.3803
Specimen 4	36.2783	37.1136	37.3596	40.7835	37.8836

The table 5.5 consist of value of micro hardness measurement of alloy after ageing of 8 hours at 170°C and 190° C.

**Table 5.6 Micro hardness data of composite after ageing of 8 hours**

Specimen no.	Trial 1	Trial 2	Trial 3	Trial 4	Average
Specimen 5	48.3535	47.5411	45.5996	40.11682	45.4027
Specimen 6	41.6406	43.9731	45.6856	42.8250	43.5310
Specimen 7	43.41725	40.4296	42.0495	40.1165	41.5032
Specimen 8	46.3645	49.9660	47.3995	47.3950	47.7812

The table 5.6 consist of value of micro hardness measurement of composite after ageing of 8 hours at 170°C and 190° C.

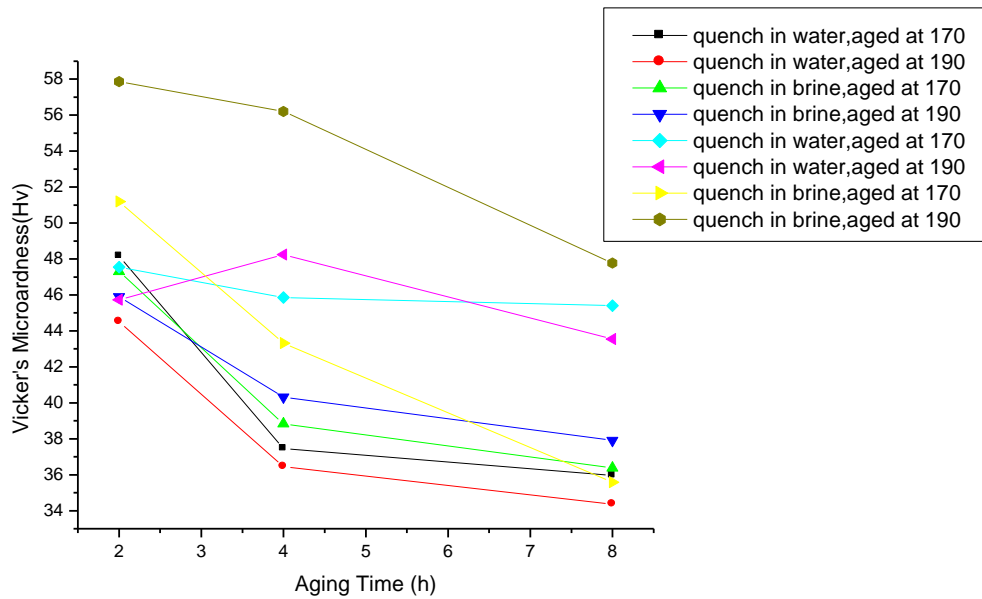


**Figure 5.1:** Micro hardness of alloys and composites as a function of aging time

In the figure 5.1 maximum micro hardness of specimen achieved after 2 hours of ageing, this could be due to uniform precipitation hardening. The graph depicts that micro hardness is decreasing after 4 hours of ageing

## 5.2 Wear Test

A pin-on-disc tribometer is used to perform the wear experiment. The alloy and composite specimens are cleaned thoroughly with acetone. Each specimen is then weighed using a Digital balance having an accuracy of  $\pm 0.1$  mg. After that the specimen is mounted on the pin holder of the tribometer ready for wear test. For all experiments, the sliding speed is adjusted to 1 m/s.

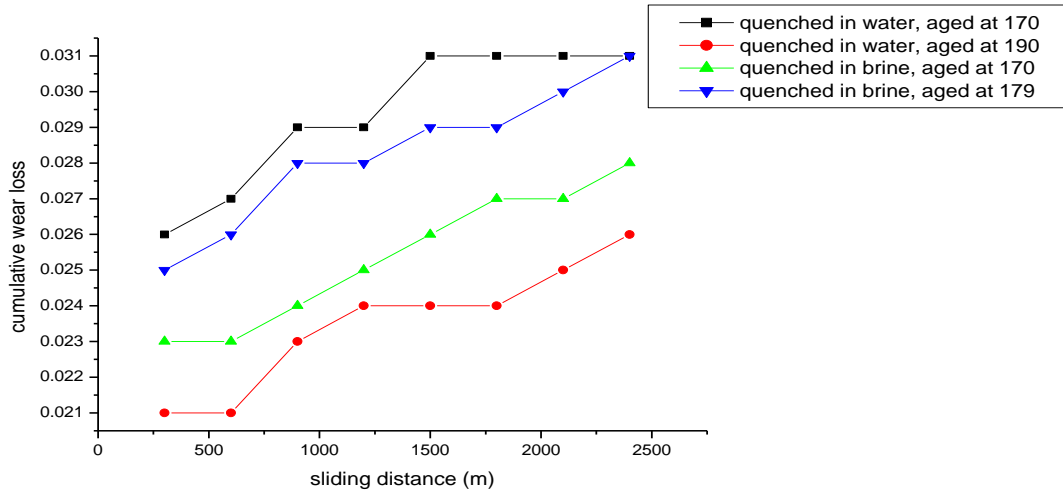


**Figure 5.2:** Cumulative wear loss of alloy as a function of sliding distance

The graph in figure 5.2 shows the cumulative wear loss of alloy specimen after solution treatment at 535°C and then quenched in water and brine solution. After quenching the specimens, ageing is done at 170°C and 190°C for 2 hours. It depicts that wear loss is increasing, when the sliding distance is increases.

**Table 5.7 Data of cumulative wear loss of alloy**

Sliding distance (m)	Wear loss of S1	Wear loss of S2	Wear loss of S3	Wear loss of S4
<b>300</b>	0.026	0.021	0.023	0.025
<b>600</b>	0.027	0.021	0.023	0.026
<b>900</b>	0.029	0.023	0.024	0.028
<b>1200</b>	0.029	0.024	0.025	0.028
<b>1500</b>	0.031	0.024	0.026	0.029
<b>1800</b>	0.031	0.024	0.027	0.029
<b>2100</b>	0.031	0.025	0.027	0.030
<b>2400</b>	0.031	0.026	0.028	0.031

**S1** = alloy quenched in water, aged at 170° C

**S2** = alloy quenched in water, aged at 190° C

**S3** = alloy quenched in brine, aged at 170° C

**S4** = alloy quenched in brine, aged at 190° C

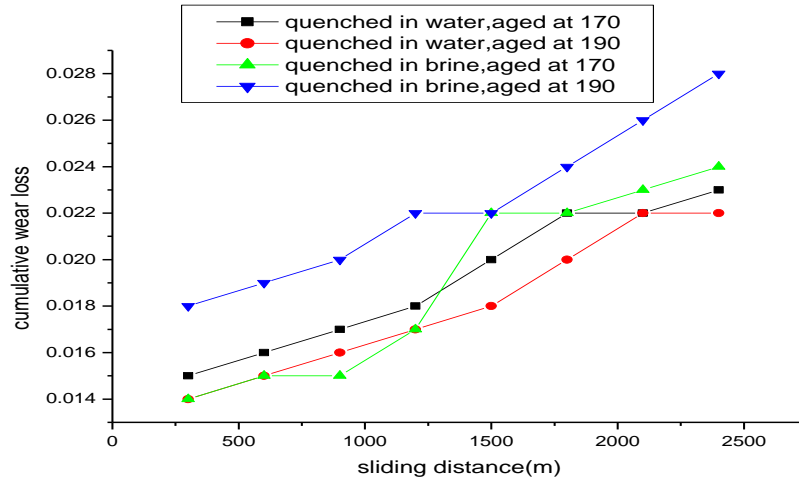


**Figure 5.3:** Cumulative wear loss of composite as a function of sliding distance

The graph in figure5.3 shows the cumulative wear loss of composite specimen after solution treatment at 535°C and then quenched in water and brine solution. After quenching the specimens, ageing is done at 170°C and 190°C for 2 hours. It depicts that wear loss is increasing, when the sliding distance is increases.

**Table 5.8 Data of cumulative wear loss of composite**

Sliding distance (m)	Wear loss of S5	Wear loss of S6	Wear loss of S7	Wear loss of S8
300	0.015	0.014	0.014	0.018
600	0.016	0.015	0.015	0.019
900	0.017	0.016	0.015	0.020
1200	0.018	0.017	0.017	0.022
1500	0.020	0.018	0.022	0.022

<b>1800</b>	0.022	0.020	0.022	0.024
<b>2100</b>	0.022	0.022	0.023	0.026
<b>2400</b>	0.023	0.022	0.024	0.028

**S5** = composite quenched in water, aged at 170° C

**S6** = composite quenched in water, aged at 190° C

**S7** = composite quenched in brine, aged at 170° C

**S8** = composite quenched in brine, aged at 190° C

### 5.3 Optical Micrography

Microstructure was visualized with the help of optical microscope. For the specimen preparation, first of all specimen were cut down then the specimen grinded on different grit size paper sequencelly by 100,220,400 and 600. After grinding, the specimens were polished by alumina paste and then etched in etchant (kellars reagant). The specimens were visualized on different magnifications.

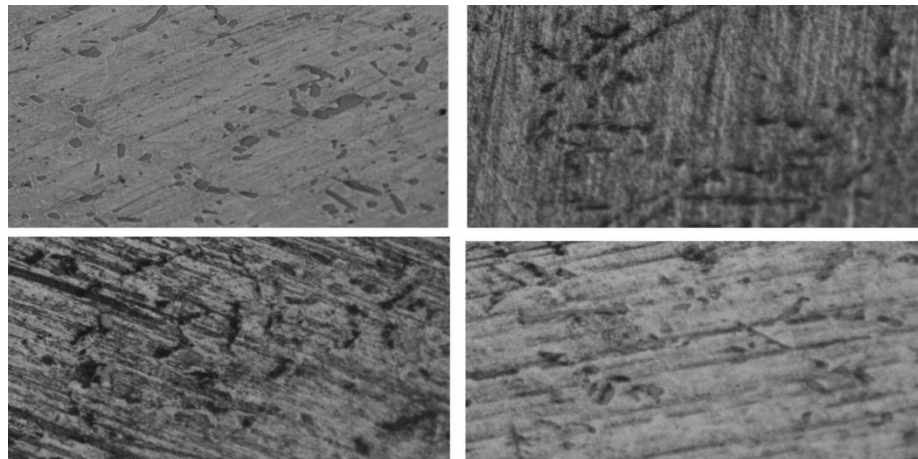


**Figure 5.4:** Microstructure image of aluminium matrix at different magnifications

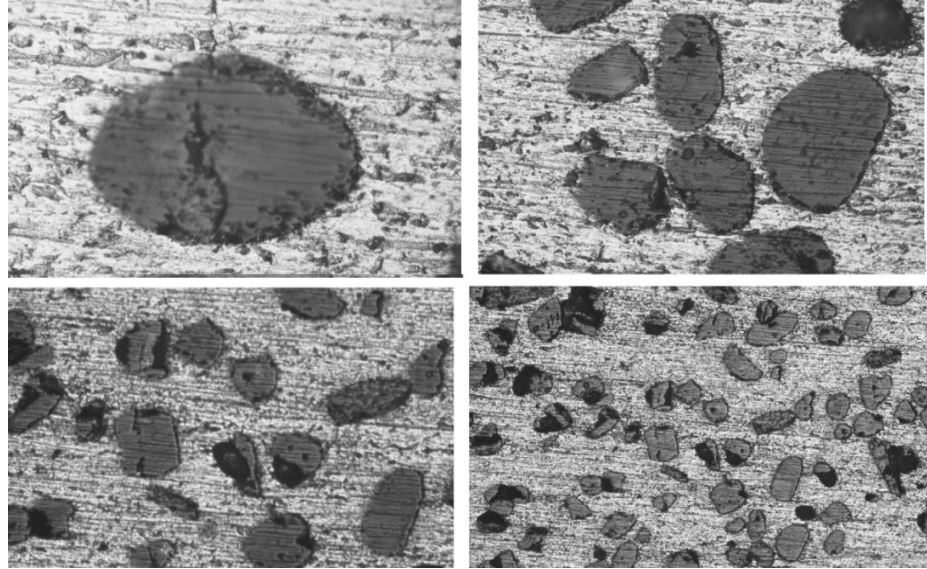


**Figure 5.5** Microstructure image of aluminium matrix embedded with zircon sand particles at different magnification

#### **5.4 SEM Results**

The cleaned and dried specimens is prepared and subsequently mounted on specially designed aluminium stubsusing. The specimens thus mounted were viewed under Jeol, JSM 6510LV scanning microscope at an accelerating voltage of 20 kV. Figure 5.6 and Figure 5.7 shows the SEM micrograph of the Aluminium alloy and Aluminium matrix composite.

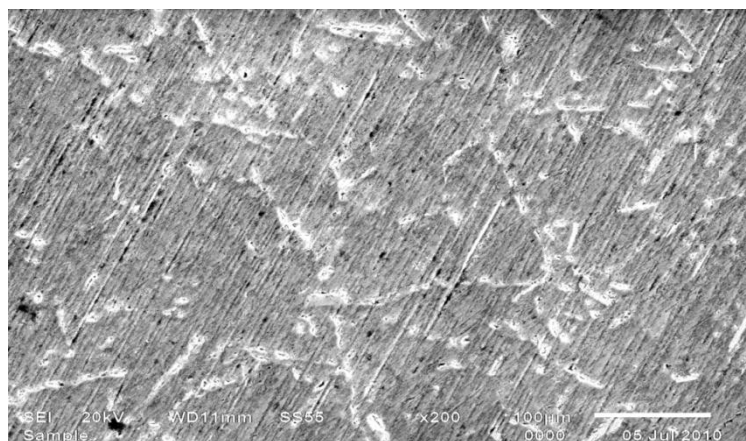


**Figure 5.6:** Scanning electron micrograph of alloy without reinforcement

It is visible that Aluminium alloy containing silicon having dendrite growth which is randomly oriented and the direction of growth of silicon is not uniform. Figure 5.6 shows a typical SEM image of Aluminium alloy without reinforcement. The Aluminium alloy containing silicon has a relatively straight morphology and non uniform of length  $42.57\mu\text{m}$ .

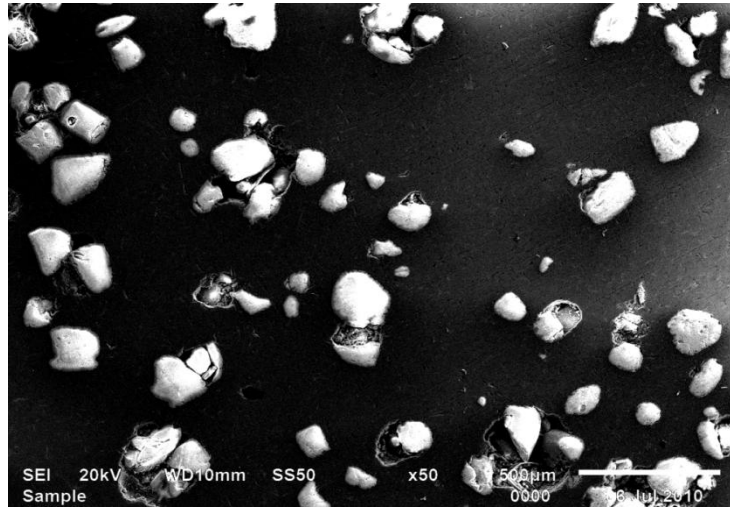


**Figure 5.7** Scanning electron micrograph of alloy with reinforcement of zircon sand

It is visible that Aluminium alloy embedded with zircon sand which is uniformly dispersed. Figure 5.7 shows a typical SEM image of Aluminium alloy with reinforcement. The Aluminium alloy embedded zircon sand has average diameter of  $90.26\mu\text{m}$ .

## 5.5 X-ray Diffraction

An X-ray powder diffraction (XRD) pattern of aluminium alloy and aluminium matrix composite is shown in Figure 5.8 and Figure 5.9. X-ray diffraction of the aluminium alloy was carried out using X'PERT PRO of PAN ANALYTICAL

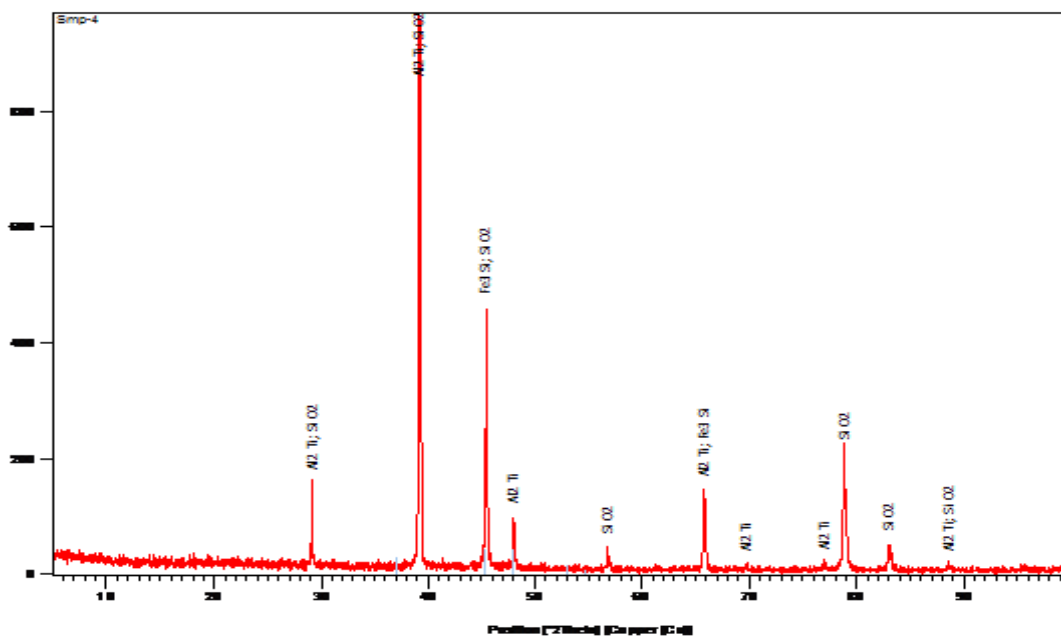


**Figure 5.8:** X-ray diffraction pattern of the alloy

**Table 5.9** XRD results of alloy

Pos. [ $^{\circ}2\text{Th.}$ ]	Rel. Int. [%]	Assignment
29.1719	14.95	$\text{Al}_2\text{Ti}$
39.1707	100.00	$\text{Al}_2\text{Ti}$
45.4132	46.95	$\text{Fe}_3\text{Si}$
47.9868	9.45	$\text{Al}_2\text{Ti}$
56.7790	4.04	$\text{SiO}_2$
65.7388	14.36	$\text{Al}_2\text{Ti}$ , $\text{Fe}_3\text{Si}$
69.7533	0.68	$\text{Al}_2\text{Ti}$
77.0512	1.17	$\text{Al}_2\text{Ti}$
78.8463	21.04	$\text{SiO}_2$
82.9773	4.63	$\text{SiO}_2$
88.6614	1.04	$\text{Al}_2\text{Ti}$ , $\text{SiO}_2$

In X-ray diffraction (Figure. 5.8), nine peaks have been obtained in the  $2\theta$  span ranging from 10 to 100. Applying extinction rules, these peaks and associated d-values have been found to correspond to the aluminium matrix composite are given in Table 5.9. The peaks in the pattern can be indexed to a mixture of different compounds, minor peaks attributed to impurity. The XRD patterns showing the intermetallic compounds in the specimen.

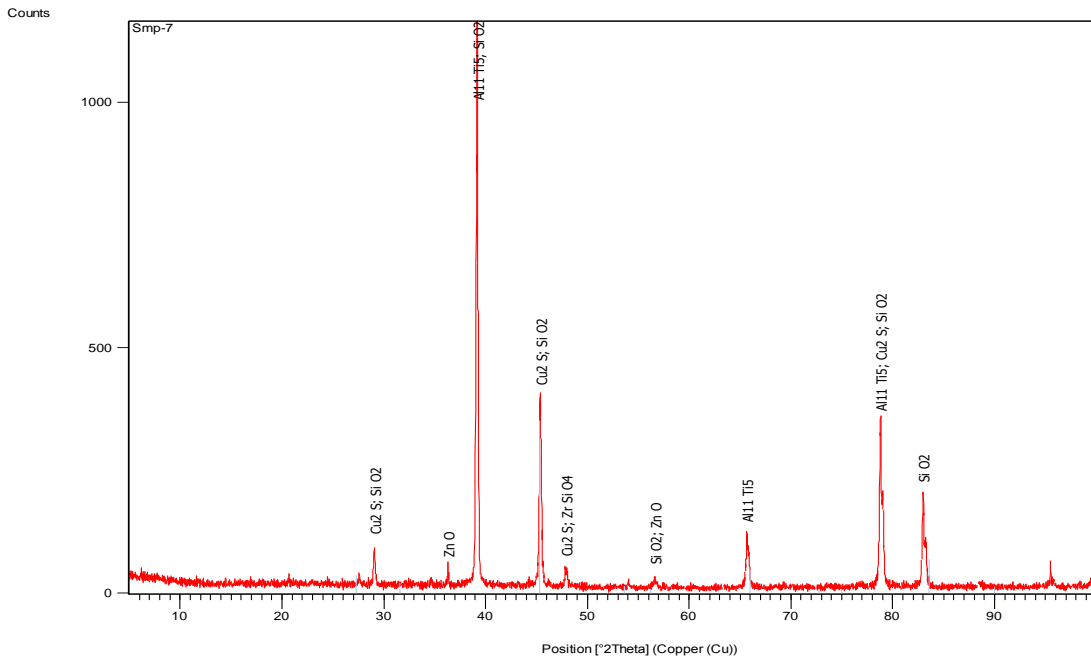


**Figure 5.9** X-ray diffraction pattern of the alloy with zircon sand

**Table 5.10** XRD results of alloy reinforced with zircon sand

Pos. [ $^{\circ}2\theta$ .]	Rel. Int. [%]	Assignment
29.0602	6.64	$\text{Cu}_2 \text{S}$ , $\text{Si O}_2$
36.3360	2.75	$\text{Zn O}$
39.1933	100.00	$\text{Al}_{11} \text{Ti}_5$ , $\text{Si O}_2$

45.3558	33.30	Cu <sub>2</sub> S, Si O <sub>2</sub>
47.9068	2.82	Cu <sub>2</sub> S, Zr Si O <sub>4</sub>
56.6607	1.60	Si O <sub>2</sub> , Zn O
65.6795	9.15	Al <sub>11</sub> Ti <sub>5</sub>
78.7939	28.70	Al <sub>11</sub> Ti <sub>5</sub> , Cu <sub>2</sub> S, Si O <sub>2</sub>
82.9480	16.22	Si O <sub>2</sub>

In X-ray diffraction (Figure. 5.9), nine peaks have been obtained in the 2θ span ranging from 10 to 100. Applying extinction rules, these peaks and associated d-values have been found to correspond to the aluminium matrix composite are given in Table 5.10. The peaks in the pattern can be indexed to a mixture of different compounds, minor peaks attributed to impurity.

### 5.6 Comparison between hardness and cumulative wear loss

The graph in figure 5.10 showing the comparison between micro hardness and cumulative wear loss. In the graph it is clearly visible that when hardness is less, wear loss is more but when the hardness increases the wear loss is decreasing.

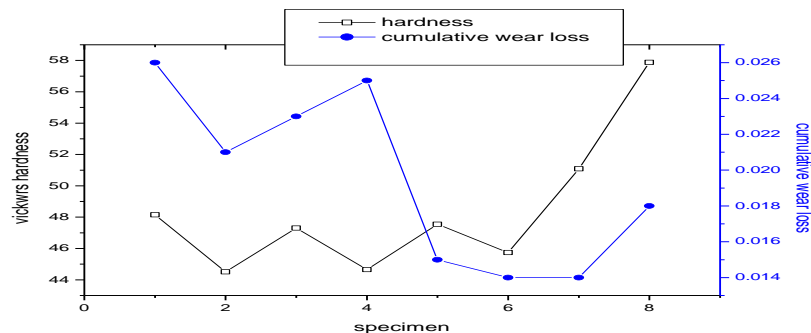


**Figure 5.10** Comparison showing relation between hardness and cumulative wear loss.

### 5.7 Area fraction of specimen by image j software

Area fraction of particle in matrix alloy of specimen 6 to know the effect of area fraction of particle on material behavior.

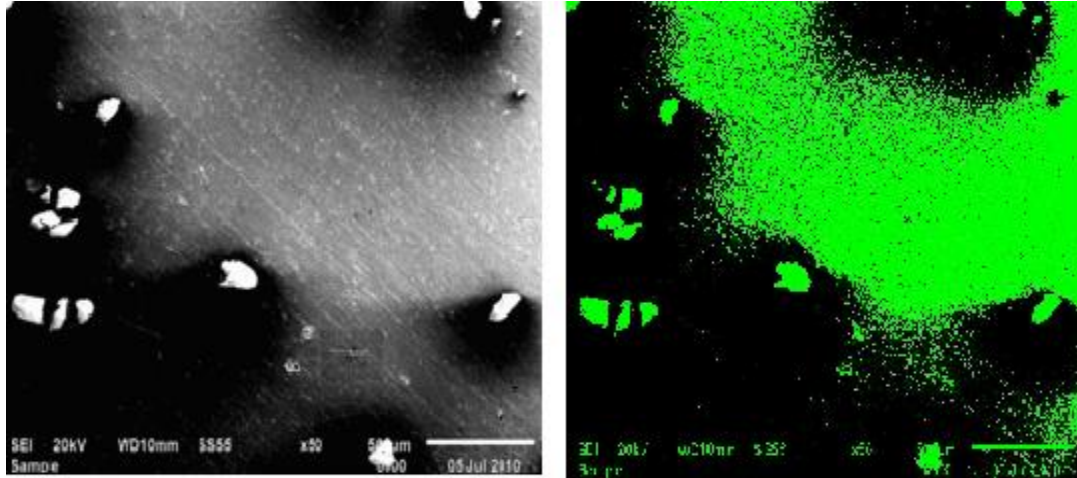


**Figure 5.11** Images of specimen 5 using image j software

The image of specimen 5 which is showing the area fraction of particle in matrix alloy is 36.9

Area fraction of particle in matrix alloy of specimen 6 to know the effect of area fraction of particle on material behavior.

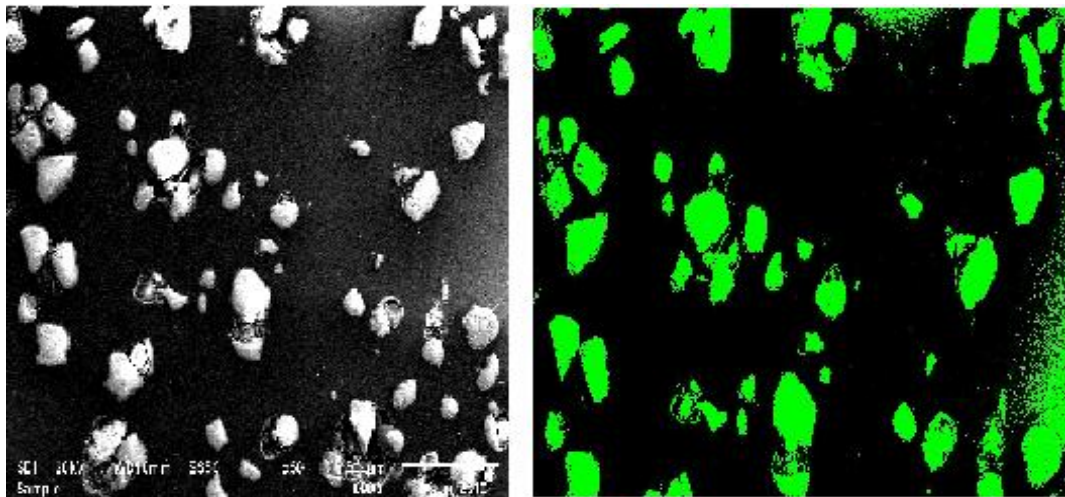


**Figure 5.12** Images of specimen 6 using image j software

The image of specimen 6 which is showing the area fraction of particle in matrix alloy is 18.4.

Area fraction of particle in matrix alloy of specimen 6 to know the effect of area fraction of particle on material behavior.

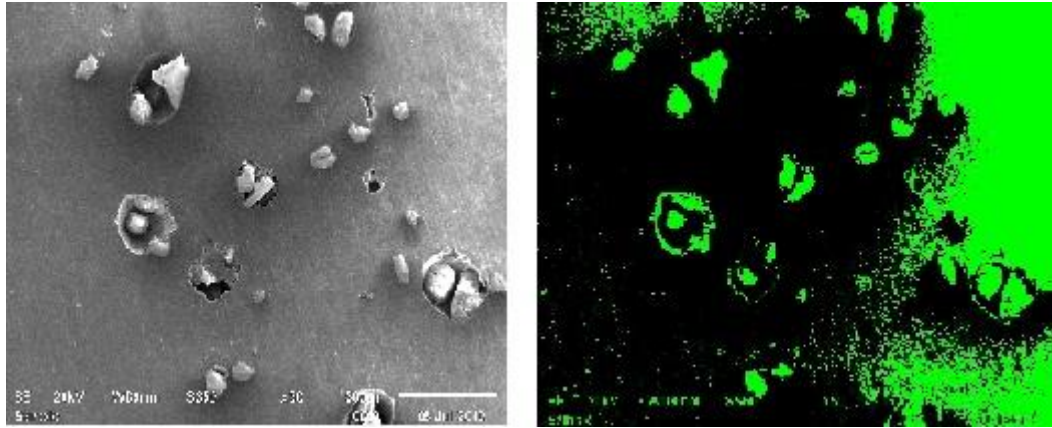


**Figure 5.11** Images of specimen 8 using image j software

The image of specimen 7 which is showing the area fraction of particle in matrix alloy is 26.8.

Area fraction of particle in matrix alloy of specimen 8 to know the effect of area fraction of particle on material behavior.

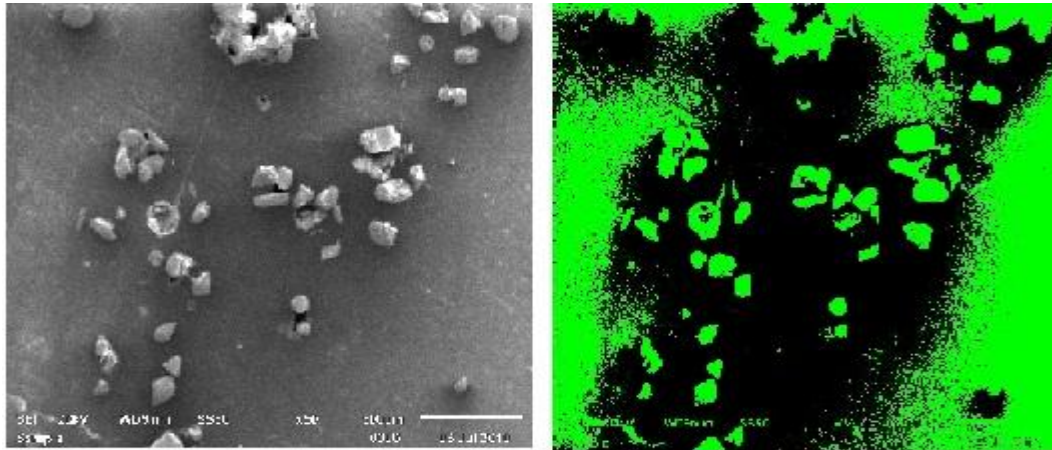


**Figure 5.14** Images of specimen 8 using image j software

The image of specimen 8 which is showing the area fraction of particle in matrix alloy is 40.1.

Comparison between slope of cumulative wear loss of composite specimen and area fraction of particle in matrix.

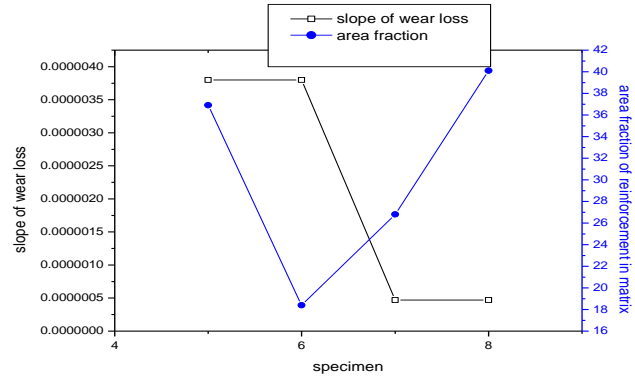


**Figure 5.15** Comparison between area fraction and slope of cumulative wear loss

In the figure 5.15, it is observed that slope of wear loss is increase, when the area of fraction of particle is less and after that wear loss is decreasing when the area fraction of particle is increasing.

## CONCLUSIONS

---

From the experiments conducted following conclusions have been obtained

1. The synthesis of aluminium alloy LM4/zircon sand can be done by stir casting route.
2. Optical micrography shows that zircon sand particle is uniformly distributed in aluminium alloy matrix.
3. The SEM reveals that zircon particles are well distributed in alloy matrix
4. XRD results showed the presence zircon particles in alloy matrix.
5. The micro hardness increases after reinforcement of zircon sand particle.
6. Rate of Wear loss decreases after addition of zircon particles.
7. For synthesizing of composite by stir casting process, stirrer design and position, stirring speed and time, particle-preheating temperature, particle incorporation rate, are the important process parameters.
8. Comparison between micro hardness and wear loss shows that hardness is less when wear loss is more. Area fraction of reinforcement in matrix affects the wear loss of composite.

## REFERENCES

---

- [1] N.Chawla and K.K. Chawla, *Metal Matrix Composites*, Springer, 10 0-387 233067
- [2] Karl Ulrich Kainer, *Metal Matrix Composites. Custom-made Materials for Automotive and Aerospace Engineering*, Wiley-Vch, 3-527-31360-5
- [3] Anthony Kelly, Karl Zweben, *Comprehensive composite materials: design and application*, Elsevier, volume 6, ISBN-0-08-043724-9
- [4] T. V. Ranjan, C.P. Sharma, Ashok Sharma, *Heat Treatment Principles and techniques*, Prentice Hall India, ISBN-81-203-0716-X
- [5] BANERJI, S. V. PRASAD, M. K SURAPPA and P. K. ROHATGI, *Abrasive wear of cast aluminium alloy-zircon composite*, Regional Research Laboratory, Council of Scientific and Industrial Research, 82 (1982) 141 – 151
- [6] Sanjeev Das, V. Udhayabanu, S. Das, K. Das, *Synthesis and characterization of zircon sand/Al-4.5 wt% Cu composite produced by stir casting route*, J Mater Sci (2006) 41:4668–4677
- [7] Sanjeev Das S. Das K. Das, *Ageing behavior of Al–4.5 wt% Cu matrix alloy reinforced with Al<sub>2</sub>O<sub>3</sub> and ZrSiO<sub>4</sub> particulate varying particle size*, J Mater Science 41(2006) 5402–5406.
- [8] Sanjeev Das, Siddhartha Das, Karabi Das, *Abrasive wear of zircon sand and alumina reinforced Al-4.5 wt% Cu alloy matrix composites – A comparative study*, composites Science and Technology 67 (2007) 746-751
- [9] L. Pederson, L. Arnberg, *The effect of solution heat treatment and quenching rates on mechanical properties and microstructures in Al-Si-Mg foundry alloys*, Metallurgical and materials transactions A 32A, march 2001—527
- [10] Ashutosh Sharma, Sanjeev Das, *Study of age hardening behavior of Al–4.5 wt% Cu/zircon sand composite in different quenching media – A comparative study* Materials and Design 30 (2009) 3900–3903.

- [11] Lin Geng, Hong-yu Xu, Kuai Yu and Hong-lin Wang, *Aging behavior of Al<sub>2</sub>O<sub>3</sub> short fiber reinforced Al-Cu alloy composites*, The Nonferrous Metals Society of China vol. 17, issue 5, oct. (2007)1018-1021.
- [12] Y. Sahin, *Preparation and some properties of SiC particle reinforced aluminium alloy composites*, Materials and Design vol. 24 (2003) 671–679.
- [13] L.A. Dobrzanski, L. Reimann, G. Krawczyk, *Influence of the Ageing on Mechanical Properties of the Aluminium Alloy AlSi9Mg*, Archives of Materials Science and Engineering vol. 31, may 2008, 37-40.
- [14] S.B. Hassan, V.S. Aigbodion, *The effect of thermal ageing on microstructure and mechanical properties of Al–Si–Fe/Mg alloys*, Journal of Alloys and Compounds, Volume 486, Issues 1-2, 3 November 2009, 309-314.
- [15] M.M. Sharma, M.F. Amateau, T.J. Eden, *Aging response of Al–Zn–Mg–Cu spray formed alloys and their metal matrix composites*, Materials Science and Engineering: A, Volume 424, Issues 1-2, 25 May 2006, 87-96.
- [16] Sharmilee Pal, R. Mitra, V.V. Bhanuprasad, *Aging behaviour of Al–Cu–Mg alloy–SiC composites*, Materials Science and Engineering: A, Volume 480, Issues 1-2, 15 May 2008, 496-505.
- [17] R.N. Rao, S. Das, *Effect of matrix alloy and influence of SiC particle on the sliding wear characteristics of aluminium alloy composites*, Materials and Design (2009)
- [18] Sharma Rajesh, Anesh, Dwivedi D. K., *Solutionizing temperature and abrasive wear behaviour of cast Al-Si-Mg alloys*, vol. 28, no6, 2007, 1975-1981
- [19] T V S Reddy, D K Dwivedi, N K Jain, *Effect of stir casting on the microstructure and adhesive wear characteristic of cast Al-Si-Cu alloy*, vol. 223, no 1,2009, 083-087
- [20] Manchang Gui1, Peiyong Li, Jianmin Han , *Fabrication and characterization of cast magnesium matrix composites by vacuum stir casting process*, Volume 12, Number 2 / April, 2003, 128-134
- [21] Peng Yu, C.K. Kwok, C.Y. To, T.K. Li, Dickon H.L. Ng, *Enhanced precipitation hardening in an alumina reinforced Al–Cu alloy matrix composite*, Composites: Part B 39 (2008) 327–331.

- [22] Yahya Altunpak, Hakem Akbulut, *Effects of aging heat treatment on machinability of alumina short fiber reinforced LM 13 aluminium alloy*, Volume 43, Numbers 5-6 / July, 2009, 449-454.
- [23] [www.wikipedia.com](http://www.wikipedia.com)
- [24] [www.substech.com](http://www.substech.com)